

# 000 TVNET: A NOVEL TIME SERIES ANALYSIS METHOD 001 002 BASED ON DYNAMIC CONVOLUTION AND 3D- 003 VARIATION 004

005  
006 **Anonymous authors**  
007 Paper under double-blind review  
008  
009  
010

## 011 ABSTRACT 012

013 With the recent development and advancement of Transformer and MLP archi-  
014 tectures, significant strides have been made in time series analysis. Conversely,  
015 the performance of Convolutional Neural Networks (CNNs) in time series analy-  
016 sis has fallen short of expectations, diminishing their potential for future applica-  
017 tions. Our research aims to enhance the representational capacity of Convolutional  
018 Neural Networks (CNNs) in time series analysis by introducing novel perspec-  
019 tives and design innovations. To be specific, We introduce a novel time series  
020 reshaping technique that considers the inter-patch, intra-patch, and cross-variable  
021 dimensions. Consequently, we propose **TVNet, a dynamic convolutional net-**  
022 **work leveraging a 3D perspective to employ time series analysis.** TVNet re-  
023 tains the computational efficiency of CNNs and achieves state-of-the-art results in  
024 five key time series analysis tasks, offering a superior balance of efficiency and  
025 performance over the state-of-the-art Transformer-based and MLP-based models.  
026 Additionally, our findings suggest that TVNet exhibits enhanced transferability  
027 and robustness. Therefore, it provides a new perspective for applying CNN in  
028 advanced time series analysis tasks.  
029

## 030 1 INTRODUCTION 031

032 Time series analysis plays a crucial role in many domains(Alfares & Nazeeruddin, 2002), such as  
033 anomaly detection(Pang et al., 2021) in industry signal and generation predication of renewable en-  
034 ergy sources(Zhang et al., 2014). In recent years, remarkable progress has been made in this area(Wu  
035 et al., 2022a),(Luo & Wang, 2024). In particular, the MLP-based and Transformer-based architec-  
036 ture show excellent performance and outstanding potential when processing time series data(Wu  
037 et al., 2021),(Zhou et al., 2022),(Zhou et al., 2021),(Wu et al., 2022b),(Li et al., 2023a),(Challu  
038 et al., 2023). **Although the convolutional neural network (CNN) has proved its powerful func-**  
039 **tion in image and video processing, its application and research in time series predication and**  
040 **analysis are relatively limited.**

041 Time series data differ from other types of sequential data(Lim & Zohren, 2021), such as language or  
042 video, in that they are continuously recorded, with only a few scalar values stored at each time stamp.  
043 Because a single time stamp typically lacks sufficient information for comprehensive analysis, many  
044 studies focus on changes between time stamps. These changes often contain more information,  
045 better reflecting the continuity, periodicity, and trends inherent in time series data. However, real-  
046 world time series often exhibit complex temporal patterns where multiple types of changes such as  
047 increases, decreases, and fluctuations are intertwined, making it challenging to model these temporal  
048 dynamics effectively.

049 Modeling one-dimensional time variations can be a complex task due to the intricate patterns in-  
050 volved. Despite these challenges, researchers have made significant progress in this area, though  
051 the most effective method for modeling time variations remains an open question. It is important to  
052 recognize that real-world time series often exhibit complex characteristics, necessitating a thorough  
053 analysis that accounts for short-term fluctuations, long-term trends, and temporal pattern changes.  
Concurrently, the cross-variable dependencies within multivariate time series must be considered.

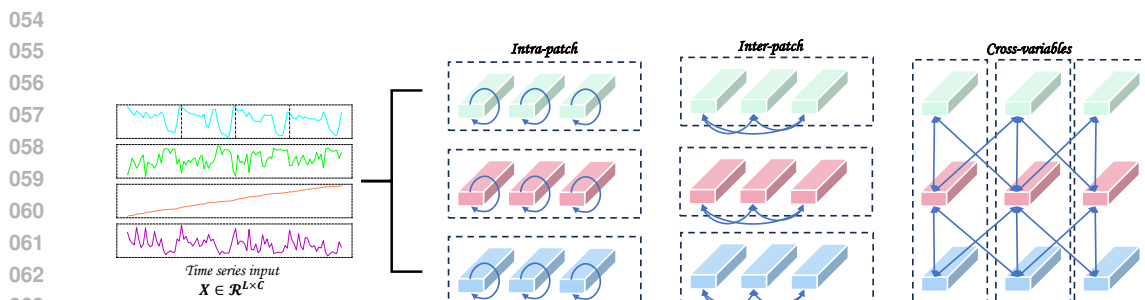


Figure 1: In the context of time series analysis, the three-dimensional variation encompasses **intra-patch**, **inter-patch**, and **cross-variable** interactions.

Furthermore, convolution is a potentially effective method for capturing cross-variable dependencies, which are essential in time series analysis alongside cross-time dependencies.(Lai et al., 2018) These dependencies pertain to the relationships among variables within multivariate time series. Although previous studies have considered modeling cross-variable dependencies via convolution,((Luo & Wang, 2024)) the distinct characteristics of variables in time series tasks have not been adequately addressed in terms of their lead or lag relationships. As described above, we assume that a judicious design of the convolution structure can uniformly model the intra-patch, inter-patch, and cross-variable(Figure 1) dependencies across different variables.

Motivated by the above considerations, we introduce a novel analytical approach within the realm of time series analysis by integrating dynamic convolution. Specifically, we introduce a 3D-Embedding technique to convert one-dimensional time series tensors into three-dimensional tensors. Subsequently, we propose a network architecture, termed TVNet, which leverages dynamic convolution to effectively capture inter-patch, intra-patch, and cross-variable dependencies for comprehensive time series analysis. We assessed the performance of TVNet across five benchmark analytical tasks: long-term and short-term forecasting, imputation, classification, and anomaly detection. Notably, despite being a purely convolution-based model, TVNet consistently achieves state-of-the-art results in these domains. Importantly, TVNet retains the efficiency inherent to dynamic convolution models, thereby achieving a superior balance between efficiency and performance, providing a practical and effective solution for time series analysis. **Our contributions are as follows:**

- A novel modeling approach that captures intra-patch, inter-patch and cross-variables features by converting 1D time series data into 3D shape tensor is proposed.
- TVNet implements consistent state-of-the-art performance time series analysis tasks across multiple mainstreams, demonstrating excellent task generalization.
- TVNet offers a better balance between efficiency and performance. It maintains the efficiency benefits of convolution based models while competing or even better with the most advanced base models in terms of performance.

## 2 RELATED WORK

### 2.1 TIME SERIES ANALYSIS

Traditional time series analysis methods, such as ARIMA (Anderson, 1976) and Holt-Winters models (Hyndman, 2018), despite their solid theoretical underpinnings, are insufficient for datasets exhibiting intricate temporal patterns. In recent years, deep learning approaches, particularly MLP-based and Transformer-based models, have achieved significant advancements in this domain (Li et al., 2023a; Challu et al., 2023; Liu et al., 2021; Zhang & Yan, 2023; Zhou et al., 2022; Wu et al., 2021; Liu et al., 2023). MLP-based models have garnered increasing attention in time series analysis due to their low computational complexity. For instance, the Dlinear model (Li et al., 2023a) achieves efficient time series prediction by integrating decomposition techniques with MLP. However, current MLP models still struggle with capturing multi-period characteristics of time series and the relationship between different variables. Concurrently, Transformer-based models have

108 demonstrated formidable performance in time series. Their self-attention mechanisms enable the  
 109 capture of both long-term dependencies and critical global information. Nevertheless, their scalabil-  
 110 ity and efficiency are constrained by the quadratic complexity of attention mechanisms. To mitigate  
 111 this, researchers have introduced techniques to diminish the computational load of Transformers.  
 112 For example, Pyraformer (Liu et al., 2021) enhances the model architecture with a pyramid atten-  
 113 tion design, facilitating connections across different scales. The recent PatchTST (Nie et al., 2022)  
 114 employs a block-based strategy, enhancing both local feature capture and long-term prediction accu-  
 115 racy. Despite these innovations, existing Transformer-based methods, which predominantly model  
 116 1D temporal variations, continue to encounter substantial computational challenges in long-term  
 117 time series analysis.

118 **2.2 CONVOLUTION IN TIME SERIES ANALYSIS**

119 As deep learning techniques advance, Transformer-based and MLP-based models have achieved  
 120 notable success in time series analysis, overshadowing traditional convolutional methods. Yet, in-  
 121 novative research is revitalizing convolution for time series analysis. The MICN model (Wang  
 122 et al., 2023) integrates local features and global correlations by employing a multi-scale convolution  
 123 structure. SCINet (Liu et al., 2022a) innovates by discarding causal convolution in favor of a recur-  
 124 sive downsample-convolution interaction architecture to handle complex temporal dynamics. While  
 125 these models have made strides in capturing long-term dependencies, they are challenged in the  
 126 generality of time series tasks. TimesNet (Wu et al., 2022a) uniquely transforms one-dimensional  
 127 time series into 2D forms, leveraging two-dimensional convolutional techniques from computer vi-  
 128 sion to enhance information representation. ModernTCN (Luo & Wang, 2024) extends the scope  
 129 of convolutional technology by utilizing large convolution kernels to capture global time series fea-  
 130 tures. However, these models predominantly focus on feature analysis within a single time window,  
 131 neglecting the comprehensive integration of global, local, and cross-variable interactions.

132 **2.3 DYNAMIC CONVOLUTION IN VIDEO**

133 Dynamic convolution, characterized by their adaptive weight or module adjustments, exhibit struc-  
 134 tural flexibility in response to content variations. These networks incorporate dynamic filtering or  
 135 convolution mechanisms ((Jia et al., 2016), (Yang et al., 2019)). They demonstrate superior process-  
 136 ing capabilities and enhanced performance relative to conventional static networks. In the domain  
 137 of video understanding, dynamic networks have also proven effective. For instance, dynamic filter-  
 138 ing techniques and temporal aggregation methods adeptly capture temporal dynamics within videos,  
 139 thereby augmenting the models' capacity to represent time series data.((Meng et al., 2021), (Li et al.,  
 140 2020))

141 **3 TVNET**

142 Based on the inter-patch, intra-patch, and cross-variable features of the time series mentioned above,  
 143 this paper proposes TVNet to capture the features of the time series. Specifically, we first design the  
 144 3D-embedding module so that the 1D time series can be converted to 3D time series tensor, and a 3D-  
 145 block is designed to model the three types of properties (inter-patch,intra-patch, and cross-variable)  
 146 through dynamic convolution. Finally, time series representations are extracted by 3D-blocks to get  
 147 different task outputs through the linear layer. Figure 2 shows the structure of TVNet.

148 **3.1 3D-EMBEDDING**

149 In this section, we propose a unique embedding way(**3D-Embedding**). This method takes into  
 150 account the inter-patch, intra-patch and cross-variable for time series. We denote  $X_{in} \in \mathbb{R}^{L \times C}$ ,  $L$   
 151 means the length of time series,  $C$  means the dimensions of time series.

152 We first embed the input along the feature dimensions  $C$  to  $C_m$  and get  $X_{in} \in \mathbb{R}^{L \times C_m}$ , where  $C_m$   
 153 as the embedding dimensions.Embedding dimension  $C_m$  is a crucial hyperparameter that dictates  
 154 the dimensionality of the representation space into which each time point is projected. After embed-  
 155 ding the input data along the feature dimension to obtain  $X_{in} \in \mathbb{R}^{L \times C_m}$ , we proceed to segment the  
 156 embedded data into patches using a one-dimensional convolutional layer (Conv1D). **Specifically, we**

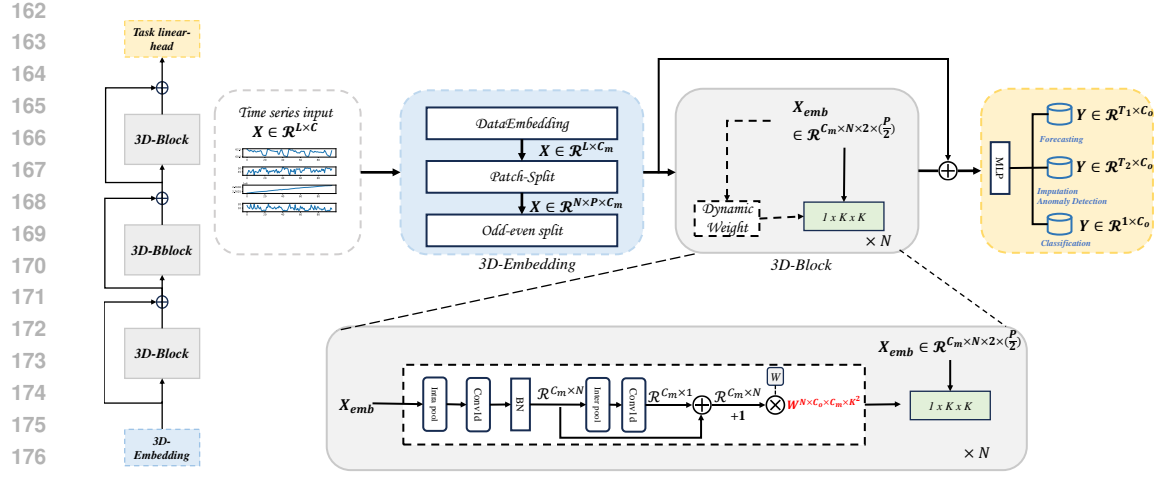


Figure 2: The overarching architecture of **TVNet** is constructed by stacking 3D-blocks in a residual way, which enables the capture of inter-patch, intra-patch, and cross-variable features from the time series 3D tensor.

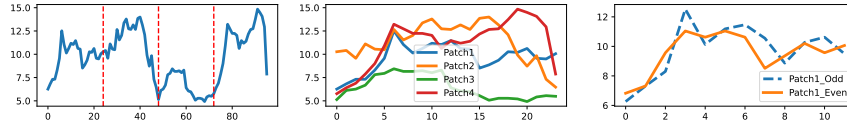


Figure 3: A univariate time series example is segmented into four distinct patches and the odd and even components specifically for Patch1 (ETTh1).

configure the Conv1D layer with a kernel size  $P$ , which defines the length of each patch. This configuration allows the Conv1D layer to divide the input sequence into  $N$  patches, where  $N$  is calculated based on the total length  $L$ , the patch length  $P$  (In the absence of overlapping patches,  $N = L/P$ ). The output of this Conv1D operation is a tensor  $X_{emb} \in \mathbb{R}^{N \times P \times C_m}$ , with each  $N$  representing the number of patches,  $P$  representing the length of each patch, and  $C_m$  representing the embedding dimensions. Then we use odd-even split(Liu et al., 2022a) on the patch length demisions to get  $X_{odd} \in \mathbb{R}^{N \times (P/2) \times C_m}$  and  $X_{even} \in \mathbb{R}^{N \times (P/2) \times C_m}$ , then stacking  $X_{odd}$  and  $X_{even}$  to get  $X_{emb} \in \mathbb{R}^{N \times 2 \times (P/2) \times C_m}$ . Figure 3 illustrates an example of patches and odd-even components applied to a univariate time series. (see Algorithm 1)

$$X_{emb} = \text{3D-Embedding}(X_{in}) \quad (1)$$

### 3.2 3D-BLOCK

**Time dynamic weight:** Previous research, as detailed in Wang et al. (2023), has highlighted both consistencies and discrepancies within time series data, particularly in the phenomenon known as mode drift. In response to these observations and inspired by dynamic convolution work in the video field(Huang et al., 2021), Regarding the 3D-Embedding technique mentioned earlier, we employ a dynamic convolutional method to capture the temporal dynamics within each patch. To clarify, the embedded representation  $X_{emb}$  is envisioned as a collection of individual patches, denoted as  $(x_1, x_2, \dots, x_N)$ . The weight associated with the  $i$ -th patch, denoted as  $W_i$ , is hypothesized to be decomposable into the product of a constant **time base weight**  $W_b$ , which is common across all patches, and a **time varying weight**  $\alpha_i$ , which is unique to each patch.

$$\tilde{x}_i = W_i \cdot x_i = (\alpha_i \cdot W_b) \cdot x_i, \quad (2)$$

**Time varying weight generation:** To more accurately model the temporal dynamics of patches, the time-varying weight  $\alpha_i$  must account for all patches. Based on the above starting point, we design an adaptive Time-varying weight generation that fully considers the interaction between inter-patch

and intra-patch. It can be articulated as  $\alpha_i = \mathcal{G}(X_{\text{emb}})$ . Here,  $\mathcal{G}$  denotes the generation function for the time-varying weight. To efficiently handle both inter-patch and intra-patch relationships and to manage pre-training weights effectively, the weights of the 3D-block can be initialized akin to standard convolutional layers. This initialization is realized by setting the weights of  $\mathcal{F}(\mathbf{v}_{\text{inter}}) + \mathcal{F}(\mathbf{v}_{\text{intra}})$  and augmenting the formulation with a constant vector of ones(1). The Figure 8 shows the flow chart for Time varing weight generation.

$$\alpha_i = \mathcal{G}(X_{\text{emb}}) = 1 + \mathcal{F}(\mathbf{v}_{\text{inter}}) + \mathcal{F}(\mathbf{v}_{\text{intra}}) \quad (3)$$

In this way, at the initial state,  $W_i = 1 \cdot W_b$ .

The function  $\mathcal{F}(\mathbf{v}_{\text{intra}})$  captures intra-patch features. Initially, we apply 3D Adaptive Average Pooling to the embedded representation  $X_{\text{emb}}$  to obtain intra-patch description vectors  $\mathbf{v}_{\text{intra}}$ , which encapsulate the essential features of each patch. These vectors are of dimension  $\mathbb{R}^{C_m \times N}$ . This operation is described by the following equation:

$$\mathbf{v}_{\text{intra}} = \text{AdaptiveAvgPool3d}(X_{\text{emb}}) \quad (4)$$

Subsequently, for intra-patch channel modeling, we employ a single-layer Conv1D, denoted as  $\mathcal{F}_{\text{intra}}$ , on  $\mathbf{v}_{\text{intra}}$ .

$$\mathcal{F}_{\text{intra}}(\mathbf{v}_{\text{intra}}) = \delta(\text{BN}(\text{Conv1D}^{C \rightarrow C}(\mathbf{v}_{\text{intra}}))) \quad (5)$$

Here,  $\delta$  represents ReLU activation, and BN denotes Batch Normalization.

The function  $\mathcal{F}(\mathbf{v}_{\text{inter}})$  is tasked with capturing features for inter-patches. We employ Adaptive Average Pooling 1D on  $\mathbf{v}_{\text{intra}}$  to derive  $\mathbf{v}_{\text{inter}}$ . This process can be expressed as:

$$\mathbf{v}_{\text{inter}} \in \mathbb{R}^{C_m \times 1} = \text{AdaptiveAvgPool1d}(\mathbf{v}_{\text{intra}}) \quad (6)$$

Subsequently, for inter-patch channel modeling, a single-layer Conv1D, denoted as  $\mathcal{F}_{\text{inter}}$ , is applied to  $\mathbf{v}_{\text{inter}}$ :

$$\mathcal{F}_{\text{inter}}(\mathbf{v}_{\text{inter}}) = \delta(\text{Conv1D}^{C \rightarrow C}(\mathbf{v}_{\text{inter}})) \quad (7)$$

Here,  $\delta$  denotes the ReLU activation function.

### 3.3 OVERALL STRUCTURE

Following the 3D-Embedding process, the embedded representation  $X_{\text{emb}}$  can be permuted to the form  $X_{\text{emb}} \in \mathbb{R}^{C_m \times N \times 2 \times (P/2)}$ , which is then input into the 3D-block architecture. The purpose of this step is to learn effective representations of the time series, denoted as  $X^{3D} \in \mathbb{R}^{C_m \times N \times 2 \times (P/2)}$ . Subsequently,  $X^{3D}$  is reshaped into  $X \in \mathbb{R}^{(NP) \times C_m}$  and passed through linear layer, also referred to as the task-linear head, to accommodate the specific requirements of various tasks.

$$X^{3D} = \text{TVNet}(X_{\text{emb}}) \quad (8)$$

$\text{TVNet}(\cdot)$  is the stacked 3D-blocks. Each 3D-block is organized in a residual way. The forward process in the  $i$ -th 3D block is:

$$X_{i+1}^{3D} = \text{3D-block}(X_i^{3D}) + X_i^{3D} \quad (9)$$

where  $X_i^{3D} \in \mathbb{R}^{C_m \times N \times 2 \times (P/2)}$  is the  $i$ -th block's input. (see Algorithm 2)

## 4 EXPERIMENT

$\text{TVNet}$  is evaluated across five common analytical tasks, including both long-term and short-term forecasting, data imputation, classification, and anomaly detection, to demonstrate its adaptability in diverse applications.

**Baselines:** In establishing foundational models for time series analysis, we have extensively incorporated the most recent and advanced models from the time series community as benchmarks. This includes Transformer-based models such as iTransformer, PatchTST, Crossformer, and FEDformer(Liu et al., 2023; Nie et al., 2022; Zhang & Yan, 2023; Zhou et al., 2022); MLP-based models like MTS-Mixer, Dlinear RMLP, and RLinear(Li et al., 2023b; Zeng et al., 2023; Li et al., 2023a); and Convolution-based models including TimesNet, MICN, and ModernTCN(Wu et al., 2022a;

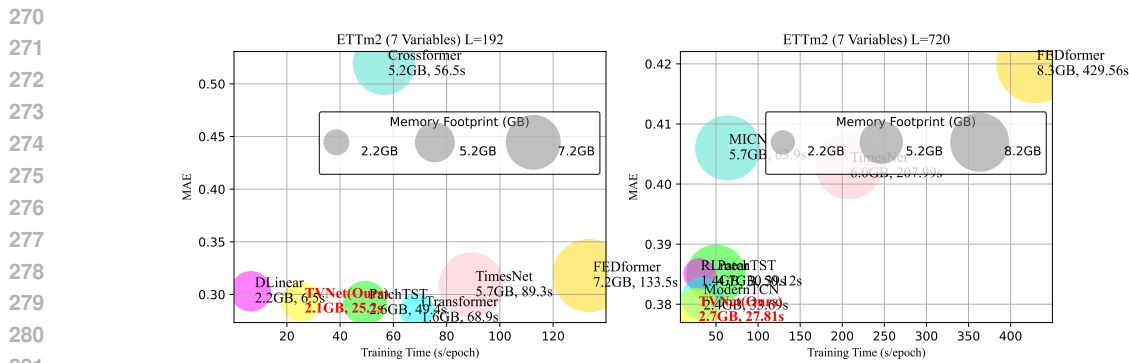


Figure 4: Model efficiency comparison under the setting of  $L$ (prediction length) = 192/720 of ETTm2.

Wang et al., 2023; Luo & Wang, 2024). Additionally, we have included state-of-the-art models from each specific task to serve as supplementary benchmarks for a comprehensive comparison. Our objective is to ensure that our model exhibits competitiveness when benchmarked against these advanced models.

**Hyperparameter Setups:** AThe performance of a model can be influenced by various hyperparameter settings. In this study, the hyperparameter ranges for TVNet are aligned with those reported in Wu et al. (2022a). A detailed discussion on the impact of each hyperparameter is provided in Appendices C and D.

**Main results:** As depicted in Figure 4, **TVNet consistently achieves top-tier performance across five pivotal analytical tasks, showcasing enhanced efficiency.** A detailed analysis of the experimental results is presented in Section 5.1. The details and outcomes of the experiments for each task are discussed in the following subsections. In the tables, the superior results are highlighted in **bold**, while those ranking just below the top are indicated with underlined.

#### 4.1 LONG-TERM FORECASTING

**Datasets and setups:** We performed long-term forecasting experiments on nine well-established real-world benchmarks: Weather(wet), Traffic(pem), Electricity(uci), Exchange(Lai et al., 2018), ILI(cdc), and four ETT datasets(Zhou et al., 2021). To ensure equitable comparison, we re-executed all baseline models with diverse input lengths, opting for the best outcomes to prevent underestimating their performance. Mean Squared Error (MSE) and Mean Absolute Error (MAE) are adopted as the metrics for evaluating multivariate time series forecast.

**Results:** Table 1 illustrates the exceptional performance of TVNet in long-term forecasting. Specifically, TVNet outperformed the majority of existing MLP-based, Transformer-based, and Convolution-based models across all nine datasets. This outcome suggests that our design significantly improves the predictive capabilities of time series forecasting via convolution.

#### 4.2 SHORT-TERM FORECASTING

**Datasets and setups:** Our benchmark for short-term forecasting is the M4 dataset, as introduced by Makridakis (Makridakis et al., 2018). We have set the input sequence length to be twice that of the forecast horizon(Wu et al., 2022a). For evaluating performance, we utilize key metrics including the Symmetric Mean Absolute Percentage Error (SMAPE), Mean Absolute Scaled Error (MASE), and Overall Weighted Average (OWA). To enhance our comparative analysis, we have incorporated models such as U-Mixer (Ma et al., 2024) and N-Hits (Challu et al., 2023).

**Results:** Table 2 presents the findings. The short-term forecasting task on the M4 dataset is notably challenging due to the varied sources and temporal dynamics of the time series data. Nevertheless, TVNet retains its top ranking in this rigorous context, demonstrating its enhanced ability for temporal analysis.

Table 1: Long-term forecasting results are averaged across four prediction lengths:  $\{24, 36, 48, 60\}$  for ILI and  $\{96, 192, 336, 720\}$  for others. Lower MSE or MAE values indicate superior performance. Refer to Table 23 in the Appendix for comprehensive results.[\(Hint:Baseline results are derived from their papers.\)](#)

Models	TVNet (Ours)	PatchTST (2022)	iTransformer (2023)	Crossformer (2023)	RLinear (2023a)	MTS-Mixer (2023b)	DLinear (2023b)	TimesNet (2022a)	MICN (2023)	ModernTCN (2024)	FEDformer (2022)	RMLP (2023a)		
Metrics	MSE	MAE	MSE	MAE	MSE	MAE	MSE	MAE	MSE	MAE	MSE	MAE		
ETTm1	Avg	<b>0.348</b> <b>0.379</b>	<b>0.351</b> <b>0.381</b>	0.407 0.410	0.431 0.443	0.358 0.376	0.370 0.395	0.357 0.379	0.400 0.450	0.383 0.406	<b>0.351</b> <b>0.381</b>	0.382 0.422	0.369 0.393	
ETTm2	Avg	<b>0.251</b> <b>0.311</b>	0.255 0.315	0.288 0.332	0.632 0.578	0.256 <b>0.314</b>	0.277 0.325	0.267 0.332	0.291 0.333	0.277 0.336	<b>0.253</b> <b>0.314</b>	0.292 0.343	0.268 0.322	
ETTh1	Avg	<b>0.407</b> <b>0.421</b>	0.413 0.431	0.454 0.447	0.441 0.465	0.408 0.421	0.430 0.436	0.423 0.437	0.458 0.450	0.433 0.462	<b>0.404</b> <b>0.420</b>	0.428 0.454	0.442 0.445	
ETTh2	Avg	0.324 0.377	0.330 0.379	0.383 0.407	0.835 0.676	<b>0.320</b> <b>0.378</b>	0.386 0.413	0.431 0.447	0.414 0.427	0.385 0.430	<b>0.322</b> <b>0.379</b>	0.388 0.434	0.349 0.395	
Electricity	Avg	0.165 0.254	<b>0.159</b> <b>0.253</b>	0.178 0.270	0.293 0.351	0.169 0.261	0.173 0.272	0.177 0.274	0.192 0.295	0.182 0.292	<b>0.156</b> <b>0.253</b>	0.207 0.321	0.161 <b>0.253</b>	
Weather	Avg	<b>0.221</b> <b>0.261</b>	0.226 <b>0.264</b>	0.258 0.278	0.230 0.290	0.247 0.279	0.235 0.272	0.240 0.300	0.259 0.287	0.242 0.298	<b>0.224</b> <b>0.264</b>	0.310 0.357	0.225 0.265	
Traffic	Avg	<b>0.396</b> <b>0.268</b>	<b>0.391</b> <b>0.264</b>	0.428 0.282	0.535 0.300	0.518 0.383	0.494 0.354	0.434 0.295	0.620 0.336	0.535 0.312	<b>0.396</b> 0.270	0.604 0.372	0.466 0.348	
Exchange	Avg	<b>0.298</b> <b>0.367</b>	0.387 0.419	0.360 0.403	0.701 0.633	0.345 0.394	0.373 0.407	<b>0.297</b>	0.378	0.416 0.443	0.315 0.404	0.302 <b>0.366</b>	0.478 0.478	0.345 0.394
ILl	Avg	<b>1.406</b> <b>0.766</b>	1.443 0.798	2.141 0.996	3.361 1.235	4.269 1.490	1.555 0.819	2.169 1.041	2.139 0.931	2.567 1.055	<b>1.440</b> <b>0.786</b>	2.597 1.070	4.387 1.516	

Table 2: The task of short-term forecasting entails evaluating performance across various sub-datasets, each with distinct sampling intervals. The results are presented as a weighted average, with lower metric values signifying enhanced performance. Full results are provided in Table 24

Models	TVNet (Ours)	PatchTST (2022)	U-Mixer (2024)	Crossformer (2023)	RLinear (2023a)	MTS-Mixer (2023b)	DLinear (2023b)	TimesNet (2022a)	MICN (2023)	ModernTCN (2024)	FEDformer (2022)	N-HiTS (2023)	
WA	SMAPE	<b>11.671</b>	11.807	11.740	13.474	12.473	11.892	13.639	11.829	13.130	<b>11.698</b>	12.840	11.927
WA	MSE	<b>1.536</b>	1.590	1.575	1.866	1.677	1.608	2.095	1.585	1.896	<b>11.556</b>	1.701	1.613
WA	OWA	<b>0.832</b>	0.851	0.845	0.985	0.898	0.859	1.051	0.851	0.980	<b>0.838</b>	0.918	0.861

### 4.3 IMPUTATION

**Datasets and setups:** The imputation task is designed to estimate missing values within partially observed time series data. Missing values are prevalent in time series due to unforeseen incidents such as equipment failure or communication errors. Given that missing values can adversely affect the performance of subsequent analyses, the imputation task holds significant practical importance.(Wu et al., 2022a) Subsequently, we concentrate on electricity and weather scenarios, which frequently exhibit data loss issues. We have chosen datasets from these domains as benchmarks, including ETT(Zhou et al., 2021), Electricity (UCI)(uci), and Weather(wet). To assess the model’s capacity under varying degrees of missing data, we randomly introduce data occlusions at ratios of  $\{12.5\%, 25\%, 37.5\%, 50\%\}$ .

**Results:** Table 3 shows TVNet’s strong imputation performance despite irregular observations due to missing values. TVNet’s top results validate its capability to capture temporal dependencies in complex scenarios. Cross-variable dependencies are key in imputation, aiding in estimating missing values when some variables are observed. Methods ignoring these, like PatchTST(Nie et al., 2022) and DLinear(Zeng et al., 2023), perform poorly in this task.

Table 3: Average results for the imputation task. Randomly masking  $\{12.5\%, 25\%, 37.5\%, 50\%\}$  time points to compare the model performance under different missing degrees.Full results can be seen in 25

Models	TVNet (Ours)	PatchTST (2022)	SCINet (2022a)	Crossformer (2023)	RLinear (2023a)	MTS-Mixer (2023b)	DLinear (2023)	TimesNet (2022a)	MICN (2023)	ModernTCN (2024)	FEDformer (2022)	RMLP (2023a)	
Metrics	MSE	MAE	MSE	MAE	MSE	MAE	MSE	MAE	MSE	MAE	MSE	MAE	
ETTm1	Avg	<b>0.018</b> <b>0.088</b>	0.045 0.133	0.039 0.129	0.041 0.143	0.070 0.166	0.056 0.154	0.093 0.206	0.027 0.107	0.070 0.182	<b>0.020</b> <b>0.093</b>	0.062 0.177	0.063 0.161
ETTm2	Avg	<b>0.022</b> <b>0.086</b>	0.028 0.098	0.027 0.102	0.046 0.149	0.032 0.108	0.032 0.107	0.096 0.208	0.022 0.088	0.144 0.249	<b>0.019</b> <b>0.082</b>	0.101 0.215	0.032 0.109
ETTh1	Avg	<b>0.046</b> <b>0.145</b>	0.133 0.236	0.104 0.216	0.132 0.251	0.141 0.242	0.127 0.236	0.201 0.306	0.078 0.187	0.125 0.250	<b>0.050</b> <b>0.150</b>	0.117 0.246	0.134 0.239
ETTh2	Avg	<b>0.039</b> <b>0.127</b>	0.066 0.164	0.064 0.165	0.122 0.240	0.066 0.165	0.069 0.168	0.142 0.259	0.049 0.146	0.205 0.307	<b>0.042</b> <b>0.131</b>	0.163 0.279	0.068 0.166
Electricity	Avg	<b>0.079</b> <b>0.194</b>	0.091 0.209	0.086 0.201	0.083 0.199	0.119 0.246	0.089 0.208	0.132 0.260	0.092 0.210	0.119 0.247	<b>0.073</b> <b>0.187</b>	0.130 0.259	0.099 0.221
Weather	Avg	<b>0.024</b> <b>0.039</b>	0.033 0.057	0.031 0.053	0.036 0.090	0.034 0.058	0.036 0.058	0.052 0.110	0.030 0.054	0.056 0.128	<b>0.027</b> <b>0.044</b>	0.099 0.203	0.035 0.060

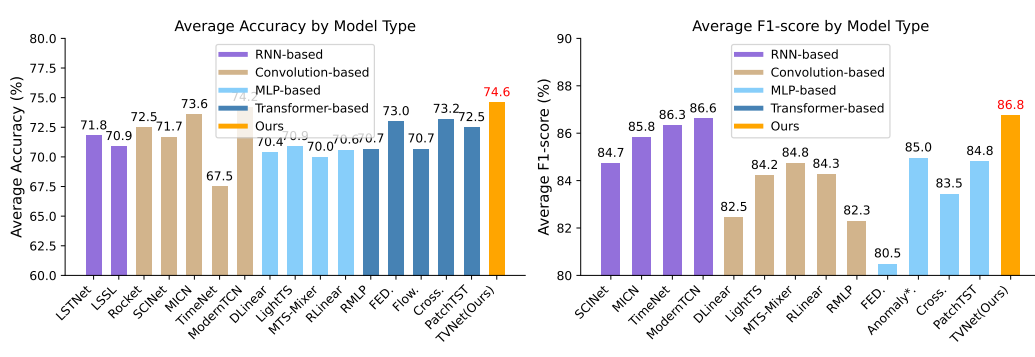


Figure 5: The results are averaged from several datasets. Higher accuracy and F1 score indicate better performance. \* in the Transformer-based models indicates the name of \*former. See Table 26 and 27 in Appendix for full results.

#### 4.4 CLASSIFICATION AND ANOMALY DETECTION

**Datasets and setups:** In our classification study, we selected 10 multivariate datasets from the UEA Time Series Classification Archive, as introduced by Bagnall (Bagnall et al., 2018) in 2018. These datasets, which serve as benchmarks, have been standardized using pre-processing practices established by Wu(Wu et al., 2022a). To ensure a comprehensive comparison, we have integrated state-of-the-art methods, including LSTNet (Lai et al., 2018), Rocket (Dempster et al., 2020), and Flowformer (Wu et al., 2022b), into our evaluation framework.

Our analysis covers a range of established benchmarks in the field of anomaly detection, including SMD (Su et al., 2019), SWaT (Mathur & Tippenhauer, 2016), PSM (Abdulaal et al., 2021), MSL, and SMAP (Hundman et al., 2018). To enhance our comparative analysis, we have incorporated the Anomaly Transformer (Xu et al., 2021) into our baseline models. Our methodology is based on the traditional approach of reconstruction, wherein the deviation from the original, measured by the reconstruction error, is the key indicator for detecting anomalies.

**Results:** The results for time series classification and anomaly detection are depicted in Figure 5. In the classification task, TVNet attained the highest performance, with an average accuracy of 74.6%. For the anomaly detection task, TVNet exhibited competitive results 86.8 relative to the previous state-of-the-art.

## 5 MODEL ANALYSIS

### 5.1 COMPREHENSIVE COMPARISON OF PERFORMANCE AND EFFICIENCY

**Summary of results:** Relative to other task-specific models and prior state-of-the-art benchmarks, TVNet has consistently achieved state-of-the-art performance across five key analytical tasks, highlighting its exceptional versatility for diverse mission types. Moreover, TVNet's efficiency, as illustrated in Figure 4, facilitates a superior balance between efficiency and performance.

**Compared with baselines:** TVNet outperforms both Transformer-based and MLP-based models in terms of performance. Concurrently, it achieves faster training speeds and lower memory usage compared to Transformer-based models, thereby demonstrating superior efficiency. TVNet's comprehensive consideration of the relationships among time series inter-patch, intra-patch, and cross-variables enhances its representational capacity over the lightweight backbone of MLP models. Compared to ModernTCN, MICN, and TimesNet, TVNet employs dynamic convolution and 3D-Embedding techniques, significantly enhancing its memory efficiency and training speed while achieving the best possible results.

**Analysis of complexity:** TVNet exhibits a time complexity of  $O(LC_m^2)$  and a space complexity of  $O(C_m^2)$ , where  $C_m$  denotes the embedding dimension. A comparison of time complexity and memory usage during training and inference phases is presented in Table 4. Relative to Transformer-

432 based models, TVNet demonstrates lower time complexity, and in contrast to convolutional models,  
 433 it maintains independence between space complexity and sequence length.  
 434

435 Table 4: Comparison of different methods in terms of training time and memory complexity.  
 436

Methods	Time Complexity	Space complexity
TVNet (Ours)	$O(LC_m^2)$	$O(C_m^2 + LC_m)$
MICN(Wang et al., 2023)	$O(LC_m^2)$	$O(LC_m^2)$
FEDformer(Zhou et al., 2022)	$O(L)$	$O(L)$
Autoformer(Wu et al., 2021)	$O(L \log L)$	$O(L \log L)$
Informer(Zhou et al., 2021)	$O(L \log L)$	$O(L \log L)$
Transformer(Liu et al., 2023)	$O(L^2)$	$O(L^2)$
LSTM	$O(L)$	$O(L)$

446  
 447 

## 5.2 ABLATION ANALYSIS

448  
 449 **Ablation of inter-pool module:** We conducted ablation experiments on the inter-pool module, and  
 450 the experimental results are shown in the Table 5. It is found in the table that when inter-pool is re-  
 451 moved, the predicted results will decrease, indicating that inter-pool can increase the representation  
 452 of the relationship between different patches.

453 Table 5: Ablation of inter-pool module in the TVNet.w/o means without module.  
 454

Models	Metrics	Weather				Electricity				Traffic			
		96	192	336	720	96	192	336	720	96	192	336	720
TVNet	MSE	0.147	0.194	0.235	0.308	0.142	0.165	0.164	0.190	0.367	0.381	0.395	0.442
	MAE	0.198	0.238	0.277	0.331	0.223	0.241	0.269	0.284	0.252	0.262	0.268	0.290
w/o inter-pool	MSE	0.156	0.211	0.247	0.349	0.147	0.178	0.186	0.199	0.377	0.399	0.410	0.458
	MAE	0.212	0.276	0.303	0.375	0.229	0.251	0.276	0.302	0.276	0.284	0.301	0.328

460 **Ablation of dynamic convolution:** Comparing the dynamic convolution weights to their fixed coun-  
 461 terparts reveals a significant decline in predictive performance without the former. This observation  
 462 underscores the effectiveness of the context-aware dynamic convolution proposed in this paper for  
 463 modeling time series analysis.(Table 6) The dynamic convolution mechanism allows for a more nu-  
 464 nanced capture of complex temporal patterns, enhancing the model’s ability to adapt to varying data  
 465 distributions and nonlinear relationships.

466 Table 6: Ablation of dynamic convolution in the TVNet.w/o means without module.  
 467

Models	Metrics	Weather				Electricity				Traffic			
		96	192	336	720	96	192	336	720	96	192	336	720
TVNet	MSE	0.147	0.194	0.235	0.308	0.142	0.165	0.164	0.190	0.367	0.381	0.395	0.442
	MAE	0.198	0.238	0.277	0.331	0.223	0.241	0.269	0.284	0.252	0.262	0.268	0.290
w/o dynamic weight	MSE	0.251	0.257	0.291	0.341	0.185	0.201	0.214	0.268	0.391	0.423	0.440	0.507
	MAE	0.226	0.269	0.301	0.370	0.275	0.296	0.308	0.316	0.306	0.313	0.311	0.327

473  
 474 

## 5.3 TRANSFER LEARNING

475 Figures 6 and 7 illustrate the outcomes of our transfer learning experiments. In both direct predic-  
 476 tion and full-tuning approaches, TVNet outperforms the baseline models, underscoring its superior  
 477 generalization and transfer capabilities. A pivotal advantage of TVNet is its dynamic weighting  
 478 mechanism, which adeptly captures intricate temporal dynamics across a variety of datasets.  
 479

480  
 481  
 482  
 483  
 484  
 485

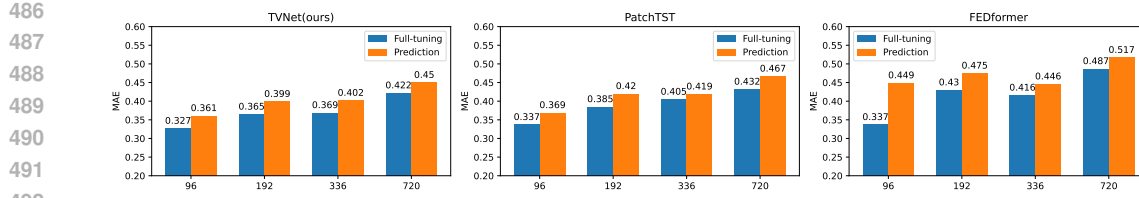


Figure 6: Transfer learning results for ETTh2.

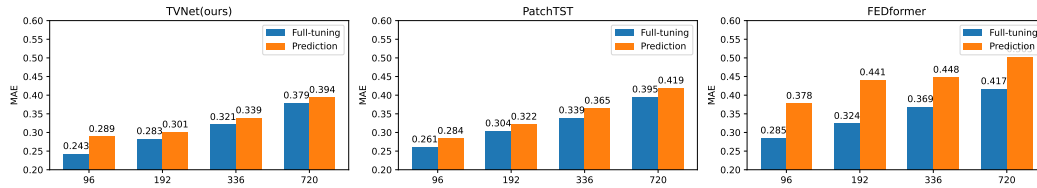


Figure 7: Transfer learning results for ETTm2.

## 6 CONCLUSION AND FUTURE WORK

This paper introduces a 3D variational reshaping and dynamic convolution method for general time series analysis. The experimental results demonstrate that TVNet exhibits excellent versatility across tasks, achieving performance comparable to or surpassing that of the most advanced Transformer-based and MLP-based models. TVNet also preserves the efficiency inherent in Convolution-based models, thus providing an optimal balance between performance and efficiency. Future research will focus on large-scale pre-training methods for time series and multi-scale patches, leveraging TVNet as the foundational architecture, which is anticipated to enhance capabilities across a broad spectrum of downstream tasks.

## REFERENCES

- Cdc. illness. URL <https://gis.cdc.gov/grasp/fluview/fluportaldashboard.html>. Accessed: 2024-08-10.
- Pems. traffic. URL <http://pems.dot.ca.gov/>. Accessed: 2024-08-10.
- Uci. electricity. URL <https://archive.ics.uci.edu/ml/datasets/ElectricityLoadDiagrams20112014>. Accessed: 2024-08-10.
- Wetterstation. weather. URL <https://www.bgc-jena.mpg.de/wetter/>. Accessed: 2024-08-10.
- Ahmed Abdulaal, Zhuanghua Liu, and Tomer Lancewicki. Practical approach to asynchronous multivariate time series anomaly detection and localization. In *Proceedings of the 27th ACM SIGKDD conference on knowledge discovery & data mining*, pp. 2485–2494, 2021.
- Hesham K Alfares and Mohammad Nazeeruddin. Electric load forecasting: literature survey and classification of methods. *International journal of systems science*, 33(1):23–34, 2002.
- Oliver D Anderson. Time-series. 2nd edn., 1976.
- Anthony Bagnall, Hoang Anh Dau, Jason Lines, Michael Flynn, James Large, Aaron Bostrom, Paul Southam, and Eamonn Keogh. The uea multivariate time series classification archive, 2018. *arXiv preprint arXiv:1811.00075*, 2018.
- Cristian Challu, Kin G Olivares, Boris N Oreshkin, Federico Garza Ramirez, Max Mergenthaler Canseco, and Artur Dubrawski. Nhits: Neural hierarchical interpolation for time series forecasting. In *Proceedings of the AAAI conference on artificial intelligence*, volume 37, pp. 6989–6997, 2023.

- 540     Angus Dempster, François Petitjean, and Geoffrey I Webb. Rocket: exceptionally fast and accu-  
 541     rate time series classification using random convolutional kernels. *Data Mining and Knowledge  
 542     Discovery*, 34(5):1454–1495, 2020.
- 543     Albert Gu, Karan Goel, and Christopher Ré. Efficiently modeling long sequences with structured  
 544     state spaces. *arXiv preprint arXiv:2111.00396*, 2021.
- 545     Ziyuan Huang, Shiwei Zhang, Liang Pan, Zhiwu Qing, Mingqian Tang, Ziwei Liu, and Marcelo H  
 546     Ang Jr. Tada! temporally-adaptive convolutions for video understanding. *arXiv preprint  
 547     arXiv:2110.06178*, 2021.
- 548     Kyle Hundman, Valentino Constantinou, Christopher Laporte, Ian Colwell, and Tom Soderstrom.  
 549     Detecting spacecraft anomalies using lstms and nonparametric dynamic thresholding. In *Pro-  
 550     ceedings of the 24th ACM SIGKDD international conference on knowledge discovery & data  
 551     mining*, pp. 387–395, 2018.
- 552     RJ Hyndman. *Forecasting: principles and practice*. OTexts, 2018.
- 553     Furong Jia, Kevin Wang, Yixiang Zheng, Defu Cao, and Yan Liu. Gpt4mts: Prompt-based large  
 554     language model for multimodal time-series forecasting. In *Proceedings of the AAAI Conference  
 555     on Artificial Intelligence*, volume 38, pp. 23343–23351, 2024.
- 556     Xu Jia, Bert De Brabandere, Tinne Tuytelaars, and Luc V Gool. Dynamic filter networks. *Advances  
 557     in neural information processing systems*, 29, 2016.
- 558     Ming Jin, Shiyu Wang, Lintao Ma, Zhixuan Chu, James Y Zhang, Xiaoming Shi, Pin-Yu Chen, Yux-  
 559     uan Liang, Yuan-Fang Li, Shirui Pan, et al. Time-lm: Time series forecasting by reprogramming  
 560     large language models. *arXiv preprint arXiv:2310.01728*, 2023.
- 561     Diederik P Kingma. Adam: A method for stochastic optimization. *arXiv preprint arXiv:1412.6980*,  
 562     2014.
- 563     Guokun Lai, Wei-Cheng Chang, Yiming Yang, and Hanxiao Liu. Modeling long-and short-term  
 564     temporal patterns with deep neural networks. In *The 41st international ACM SIGIR conference  
 565     on research & development in information retrieval*, pp. 95–104, 2018.
- 566     Yunsheng Li, Yinpeng Chen, Xiyang Dai, Dongdong Chen, Mengchen Liu, Lu Yuan, Zicheng Liu,  
 567     Lei Zhang, and Nuno Vasconcelos. Micronet: Towards image recognition with extremely low  
 568     flops. *arXiv preprint arXiv:2011.12289*, 2020.
- 569     Zhe Li, Shiyi Qi, Yiduo Li, and Zenglin Xu. Revisiting long-term time series forecasting: An  
 570     investigation on linear mapping. *arXiv preprint arXiv:2305.10721*, 2023a.
- 571     Zhe Li, Zhongwen Rao, Lujia Pan, and Zenglin Xu. Mts-mixers: Multivariate time series forecasting  
 572     via factorized temporal and channel mixing. *arXiv preprint arXiv:2302.04501*, 2023b.
- 573     Bryan Lim and Stefan Zohren. Time-series forecasting with deep learning: a survey. *Philosophical  
 574     Transactions of the Royal Society A*, 379(2194):20200209, 2021.
- 575     Minhao Liu, Ailing Zeng, Muxi Chen, Zhijian Xu, Qiuxia Lai, Lingna Ma, and Qiang Xu. Scinet:  
 576     Time series modeling and forecasting with sample convolution and interaction. *Advances in  
 577     Neural Information Processing Systems*, 35:5816–5828, 2022a.
- 578     Shizhan Liu, Hang Yu, Cong Liao, Jianguo Li, Weiyao Lin, Alex X Liu, and Schahram Dustdar.  
 579     Pyraformer: Low-complexity pyramidal attention for long-range time series modeling and fore-  
 580     casting. In *International conference on learning representations*, 2021.
- 581     Yong Liu, Haixu Wu, Jianmin Wang, and Mingsheng Long. Non-stationary transformers: Exploring  
 582     the stationarity in time series forecasting. *Advances in Neural Information Processing Systems*,  
 583     35:9881–9893, 2022b.
- 584     Yong Liu, Tengge Hu, Haoran Zhang, Haixu Wu, Shiyu Wang, Lintao Ma, and Mingsheng Long.  
 585     itransformer: Inverted transformers are effective for time series forecasting. *arXiv preprint  
 586     arXiv:2310.06625*, 2023.

- 594 Donghao Luo and Xue Wang. Moderntcn: A modern pure convolution structure for general time  
 595 series analysis. In *The Twelfth International Conference on Learning Representations*, 2024.
- 596
- 597 Xiang Ma, Xuemei Li, Lexin Fang, Tianlong Zhao, and Caiming Zhang. U-mixer: An unet-mixer  
 598 architecture with stationarity correction for time series forecasting. In *Proceedings of the AAAI  
 599 Conference on Artificial Intelligence*, volume 38, pp. 14255–14262, 2024.
- 600 Spyros Makridakis, Evangelos Spiliotis, and Vassilios Assimakopoulos. The m4 competition: Re-  
 601 sults, findings, conclusion and way forward. *International Journal of forecasting*, 34(4):802–808,  
 602 2018.
- 603
- 604 Aditya P Mathur and Nils Ole Tippenhauer. Swat: A water treatment testbed for research and  
 605 training on ics security. In *2016 international workshop on cyber-physical systems for smart  
 606 water networks (CySWater)*, pp. 31–36. IEEE, 2016.
- 607 Yue Meng, Rameswar Panda, Chung-Ching Lin, Prasanna Sattigeri, Leonid Karlinsky, Kate Saenko,  
 608 Aude Oliva, and Rogerio Feris. Adafuse: Adaptive temporal fusion network for efficient action  
 609 recognition. *arXiv preprint arXiv:2102.05775*, 2021.
- 610 Yuqi Nie, Nam H Nguyen, Phanwadee Sinthong, and Jayant Kalagnanam. A time series is worth 64  
 611 words: Long-term forecasting with transformers. *arXiv preprint arXiv:2211.14730*, 2022.
- 612
- 613 Zijie Pan, Yushan Jiang, Sahil Garg, Anderson Schneider, Yuriy Nevmyvaka, and Dongjin Song.  
 614  $s^2$  ip-lm: Semantic space informed prompt learning with llm for time series forecasting. In  
 615 *Forty-first International Conference on Machine Learning*, 2024.
- 616
- 617 Guansong Pang, Chunhua Shen, Longbing Cao, and Anton Van Den Hengel. Deep learning for  
 618 anomaly detection: A review. *ACM computing surveys (CSUR)*, 54(2):1–38, 2021.
- 619 Adam Paszke, Sam Gross, Francisco Massa, Adam Lerer, James Bradbury, Gregory Chanan, Trevor  
 620 Killeen, Zeming Lin, Natalia Gimelshein, Luca Antiga, et al. Pytorch: An imperative style, high-  
 621 performance deep learning library. *Advances in neural information processing systems*, 32, 2019.
- 622
- 623 Ya Su, Youjian Zhao, Chenhao Niu, Rong Liu, Wei Sun, and Dan Pei. Robust anomaly detection for  
 624 multivariate time series through stochastic recurrent neural network. In *Proceedings of the 25th  
 625 ACM SIGKDD international conference on knowledge discovery & data mining*, pp. 2828–2837,  
 626 2019.
- 627
- 628 Huiqiang Wang, Jian Peng, Feihu Huang, Jince Wang, Junhui Chen, and Yifei Xiao. Micn: Multi-  
 629 scale local and global context modeling for long-term series forecasting. In *The eleventh interna-  
 630 tional conference on learning representations*, 2023.
- 631
- 632 Yuxuan Wang, Haixu Wu, Jiaxiang Dong, Yong Liu, Yunzhong Qiu, Haoran Zhang, Jianmin Wang,  
 633 and Mingsheng Long. Timexer: Empowering transformers for time series forecasting with ex-  
 634ogenous variables. *arXiv preprint arXiv:2402.19072*, 2024.
- 635
- 636 Haixu Wu, Jiehui Xu, Jianmin Wang, and Mingsheng Long. Autoformer: Decomposition trans-  
 637 formers with auto-correlation for long-term series forecasting. *Advances in neural information  
 638 processing systems*, 34:22419–22430, 2021.
- 639
- 640 Haixu Wu, Tengge Hu, Yong Liu, Hang Zhou, Jianmin Wang, and Mingsheng Long. Timesnet: Tem-  
 641 poral 2d-variation modeling for general time series analysis. *arXiv preprint arXiv:2210.02186*,  
 642 2022a.
- 643
- 644 Haixu Wu, Jialong Wu, Jiehui Xu, Jianmin Wang, and Mingsheng Long. Flowformer: Linearizing  
 645 transformers with conservation flows. *arXiv preprint arXiv:2202.06258*, 2022b.
- 646
- 647 Jiehui Xu, Haixu Wu, Jianmin Wang, and Mingsheng Long. Anomaly transformer: Time series  
 648 anomaly detection with association discrepancy. *arXiv preprint arXiv:2110.02642*, 2021.
- 649
- 650 Brandon Yang, Gabriel Bender, Quoc V Le, and Jiquan Ngiam. Condconv: Conditionally parame-  
 651 terized convolutions for efficient inference. *Advances in neural information processing systems*,  
 652 32, 2019.

- 648 Ailing Zeng, Muxi Chen, Lei Zhang, and Qiang Xu. Are transformers effective for time series  
 649 forecasting? In *Proceedings of the AAAI conference on artificial intelligence*, volume 37, pp.  
 650 11121–11128, 2023.
- 651 Tianping Zhang, Yizhuo Zhang, Wei Cao, Jiang Bian, Xiaohan Yi, Shun Zheng, and Jian Li. Less is  
 652 more: Fast multivariate time series forecasting with light sampling-oriented mlp structures. *arXiv*  
 653 preprint arXiv:2207.01186, 2022.
- 654 Yao Zhang, Jianxue Wang, and Xifan Wang. Review on probabilistic forecasting of wind power  
 655 generation. *Renewable and Sustainable Energy Reviews*, 32:255–270, 2014.
- 656 Yunhao Zhang and Junchi Yan. Crossformer: Transformer utilizing cross-dimension dependency  
 657 for multivariate time series forecasting. In *The eleventh international conference on learning  
 658 representations*, 2023.
- 659 Haoyi Zhou, Shanghang Zhang, Jieqi Peng, Shuai Zhang, Jianxin Li, Hui Xiong, and Wancai Zhang.  
 660 Informer: Beyond efficient transformer for long sequence time-series forecasting. In *Proceedings  
 661 of the AAAI conference on artificial intelligence*, volume 35, pp. 11106–11115, 2021.
- 662 Tian Zhou, Ziqing Ma, Qingsong Wen, Xue Wang, Liang Sun, and Rong Jin. Fedformer: Frequency  
 663 enhanced decomposed transformer for long-term series forecasting. In *International conference  
 664 on machine learning*, pp. 27268–27286. PMLR, 2022.
- 665

## A TVNET THEORETICAL DISCUSSIONS

666 **Problem Definition: (Time Series Analysis)** Time series analysis encompasses five primary sub-  
 667 tasks: long-term forecasting, short-term forecasting, interpolation, classification, and anomaly de-  
 668 tection. Mathematically, these tasks are defined with respect to a look back window  $X \in \mathbb{R}^{L \times C}$ ,  
 669 where  $L$  is the window length and  $C$  is the number of features. The goal is to develop a deep-  
 670 learning model  $f$  that minimizes the prediction error  $e(Y, f(X))$ . The target output  $Y$  varies by  
 671 task: - For forecasting:  $Y \in \mathbb{R}^{T_1 \times C_o}$ , where  $T_1$  is the forecast horizon and  $C_o$  is the number of  
 672 output features. - For imputation and anomaly detection:  $Y \in \mathbb{R}^{T_2 \times C_o}$ , where  $T_2$  is the data length  
 673 for imputation or anomaly detection and  $C_o$  is the number of output features. - For classification:  
 674  $Y \in \mathbb{R}^{1 \times C}$ , where  $C$  represents the number of classification labels.

---

### Algorithm 1 3D-Embedding applied to general time series analysis.

---

675 **Require:** Look back window  $X \in \mathbb{R}^{L \times C}$ , where  $L$  is the length of the time series and  $C$  is the  
 676 number of channels.

677 1: Embed the input along the feature dimensions  $C$  to get  $X' \in \mathbb{R}^{L \times C_m}$ , where  $C_m$  is the embed-  
 678 ding dimension.

679 2: Use Conv1D (kernel size =  $P$ ) to divide  $X'$  into  $N$  patches  $x_i \in \mathbb{R}^{P \times C_m}$ , where  $N = \frac{L}{P}$ .

680 3: **for**  $i = 1$  to  $N$  **do**

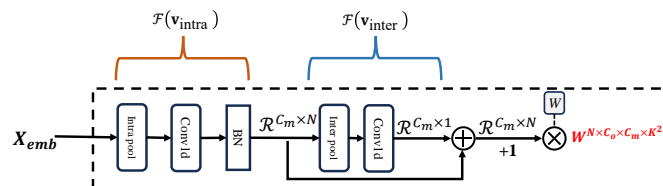
681 4:     Split each patch  $x_i$  by odd and even indices to get  $x_{odd}, x_{even} \in \mathbb{R}^{P/2 \times C_m}$ .

682 5:     Concatenate  $x_{odd}$  and  $x_{even}$  to get  $x_i \in \mathbb{R}^{2 \times (P/2) \times C_m}$ .

683 6: **end for**

684 7: Concatenate all patches to get  $X_{emb} \in \mathbb{R}^{N \times 2 \times (P/2) \times C_m}$ .

---



700 Figure 8: The Time varying weight generation flow chart

### Algorithm 2 Training of TVNet.

**Require:** **Input:** Training set  $\mathcal{D} = \{(X, Y)\}$  Look back window  $X \in \mathbb{R}^{L \times C}$ ; Embedding dimensions  $C_m$ ; number of 3D-blocks  $L$ ; Patch length  $P$  and other training hyperparameter.

**Ensure:** **Output:** Trained TVNet

1: Initialize Embedding dimensions and number of 3D-blocks.

2: Sample  $(X, Y)$  from  $\mathcal{D}$

3: (3D-Embedding):  $X_{emb} = Algorithm(X)$

4: **for** for  $i = 1$  to  $L$  do: **do**

5:       $\alpha \leftarrow$

$$6: \quad X_i^{3D} \leftarrow Conv2D(\alpha, W_b,$$

## 7: end for

8:  $Y \leftarrow \text{Ta}$

9: Compute loss  $\mathcal{L} \leftarrow \mathcal{L}(\hat{Y}, Y)$

10: Update model parameters  $\Theta$  with

11: until convergence

12: return Trained TV

#### **12. Total Framed View**

---

## A.1 THEORETICAL ANALYSIS

**Theorem B.1:** Under appropriate optimization, the dynamic weight model achieves a lower error than the fixed weight model, i.e.,  $E_d < E_f$ .

**Definition:** In the context of time series analysis, we can segment a dataset into  $N$  distinct patches, denoted as  $x_1, x_2, \dots, x_N$ , each with its corresponding true target value  $y_i^*$ . Two models are considered for processing these patches:

Fixed Weight Model: This model employs a constant weight  $W_f$  to produce the convolution output for each patch  $i$ . The output is calculated as follows:

$$y_{f,i} \equiv W_f \cdot x_i \quad (10)$$

This model uses variable weights  $W_i$  for each patch, defined as  $W_i = \alpha_i \cdot W_b$ , where  $\alpha_i$  is a coefficient that can vary with each patch. The convolution output for patch  $i$  is then given by:

$$y_{d,i} = W_i \cdot x_i = (\alpha_i \cdot W_b) \cdot x_i \quad (11)$$

*Proof:*

For the fixed weight model, the total error is given by:

$$E_f = \sum_{i=1}^N (W_f \cdot x_i - y_i^*)^2 \quad (12)$$

Expanding the square term, we get:

$$E_f = \sum_{i=1}^N ((W_f \cdot x_i)^2 - 2W_f \cdot x_i \cdot y_i^* + (y_i^*)^2) \quad (13)$$

For the dynamic weight model, the total error is given by:

$$E_d = \sum_{i=1}^N ((\alpha_i \cdot W_b \cdot x_i) - y_i^*)^2 \quad (14)$$

Expanding the square term, we get:

$$E_d = \sum_{i=1}^N ((\alpha_i \cdot W_b \cdot x_i)^2 - 2(\alpha_i \cdot W_b \cdot x_i) \cdot y_i^* + (y_i^*)^2) \quad (15)$$

756  
757  
758  
759  
760  
761

In the fixed weight model, the error  $E_f$  is minimized by optimizing the single parameter  $W_f$ :

$$\frac{\partial E_f}{\partial W_f} = 0 \Rightarrow W_f = \text{optimal fixed weight} \quad (16)$$

762 In the dynamic weight model, the error  $E_d$  is minimized by optimizing both  $W_b$  (shared across  
763 patches) and  $\alpha_i$  (specific to each patch). The optimization conditions are:

$$\frac{\partial E_d}{\partial W_b} = 0 \quad \text{and} \quad \frac{\partial E_d}{\partial \alpha_i} = 0, \forall i \quad (17)$$

764 Solving for  $\alpha_i$ :

$$\alpha_i = \frac{y_i^*}{W_b \cdot x_i}, \forall i \quad (18)$$

765 Substituting this back into  $E_d$ , the error is further reduced compared to the fixed weight model.

766 The dynamic weight model provides additional flexibility by adjusting  $\alpha_i$  for each patch  $i$ . This  
767 allows it to better approximate the target  $y_i^*$ , resulting in:

$$E_d < E_f \quad (19)$$

## 777 A.2 COMPUTATIONAL ANALYSIS:

778 Consider the input time series tensor  $X^{3D} \in \mathbb{R}^{C_m \times N \times 2 \times \frac{P}{2}}$ , where  $N \times P = L$  and  $L$  represents  
779 the time series length. Given that the output dimension of TVNet matches the input dimensions, the  
780 computational complexity for 2D convolutions can be described as follows:

$$\begin{aligned} \text{FLOPs(Conv2D)} &= C_m \times C_m \times k^2 \times N \times 2 \times (P/2) = C_m \times C_m \times k^2 \times L \\ \text{Params(Conv2d)} &= C_m \times C_m \times k^2 \end{aligned} \quad (20)$$

781  $C_m$  denote the embedding dimensions and  $k$  represent the kernel size of the 2D convolutions. In the  
782 process of generating time-varying weights, the features are initially passed through an intra-pool  
783 and subsequently through an inter-pool, which incorporates a non-parameter layer.

$$\begin{aligned} \text{FLOPs}(\mathcal{G}_{intra}) &= C_m \times N \times 2 \times P/2 = C_m \times L \\ \text{Params}(\mathcal{G}_{inter}) &= C_m \times N \end{aligned} \quad (21)$$

784 In the channel modeling process, two 1D convolutions with a kernel size of  $k = 1$  are utilized.

$$\begin{aligned} \text{FLOPs(channel)} &= C_m \times C_m \times k(1) \times N + C_m \times C_m \times k(1) \\ \text{Params(channel)} &= C_m \times C_m \times k(1) + C_m \times C_m \times k(1) \end{aligned} \quad (22)$$

785 Subsequently, the time-varying weight matrix  $\alpha \in \mathbb{R}^{C_m \times N}$  is multiplied by the temporal weight  
786 tensor  $W \in \mathbb{R}^{C_m \times C_m \times k^2}$  for 2D convolutions.

$$\text{FLOPs(multiply)} = C_m \times C_m \times k^2 \times N \quad (23)$$

787 Therefore, the total computational complexity and parameter count are as follows:

$$\begin{aligned} \text{FLOPs} &= \text{FLOPs(Conv2D)} + \text{FLOPs}(\mathcal{G}) + \text{FLOPs(channel)} + \text{FLOPs(multiply)} \\ &= C_m \times L + C_m \times L + C_m \times C_m \times k(1) \times N \\ &\quad + C_m \times C_m \times k(1) + C_m \times C_m \times k^2 \times N \end{aligned} \quad (24)$$

$$\begin{aligned} \text{Params} &= \text{Params(Conv2D)} + \text{Params}(\mathcal{G}) + \text{Params(channel)} \\ &= C_m \times C_m \times k^2 + C_m \times N + C_m \times C_m \times k(1) + C_m \times C_m \times k(1) \end{aligned} \quad (25)$$

809 Based on the computational analysis, TVNet demonstrates FLOPs of  $O(LC_m^2)$  and a parameter  
810 count of  $O(C_m^2)$ .

810      **B DATASETS**  
 811

812      **B.1 LONG-TERM FORECAST AND IMPUTATION DATASETS**  
 813

814      Assessments of the long-term forecasting capabilities were conducted using nine widely recog-  
 815      nized real-world datasets, encompassing domains such as weather, traffic, electricity, exchange  
 816      rates, influenza-like illness (ILI), and the four Electricity Transformer Temperature (ETT) datasets  
 817      (ETTh1, ETTh2, ETTm1, ETTm2). For the imputation task, benchmarks were established using  
 818      datasets from weather, electricity, and the four ETT datasets. These datasets, extensively utilized in  
 819      the field, cover various aspects of daily life.

820      The characteristics of each dataset, including the total number of timesteps, the count of variables,  
 821      and the sampling frequency, are summarized in Table 7. The datasets are partitioned into training,  
 822      validation, and testing subsets in chronological order, with the Electricity Transformer Temperature  
 823      (ETT) dataset employing a 6:2:2 ratio and the remaining datasets using a 7:1:2 ratio. Normalization  
 824      to a zero mean is applied to the training, validation, and testing subsets based on the mean and  
 825      standard deviation of the training subset. Each dataset comprises a single, continuous, long-time  
 826      series, with samples extracted using a sliding window technique.

827      Further details regarding the datasets are as follows:

- 828      1. **Weather**<sup>1</sup> consists of 21 climatic variables, such as humidity and air temperature, recorded  
   829      in Germany throughout 2020.
- 830      2. **Traffic**<sup>2</sup> includes road occupancy rates collected by 862 sensors across San Francisco Bay  
   831      area highways over a two-year period, provided by the California Department of Trans-  
   832      portation.
- 833      3. **Electricity**<sup>3</sup> comprises hourly electricity usage data for 321 consumers from 2012 to 2014.
- 834      4. **Exchange**<sup>4</sup> encompasses daily exchange rates for eight currencies, observed from 1990 to  
   835      2016.
- 836      5. **ILI**<sup>5</sup>, which stands for Influenza-Like Illness, contains weekly counts of ILI patients in the  
   837      United States from 2002 to 2021. It includes seven metrics, such as ILI patient counts  
   838      across various age groups and the proportion of ILI patients relative to the total patient  
   839      population. The data is provided by the Centers for Disease Control and Prevention of the  
   840      United States.
- 841      6. **ETT**<sup>6</sup>, The Electricity Transformer Temperature (ETT) dataset comprises data from seven  
   842      sensors across two Chinese counties, featuring load and oil temperature metrics. It includes  
   843      four subsets: 'ETTh1' and 'ETTh2' for hourly data, and 'ETTm1' and 'ETTm2' for 15-  
   844      minute intervals.

845      Table 7: Dataset descriptions of long-term forecasting and imputation.  
 846

Dataset	Weather	Traffic	Exchange	Electricity	ILI	ETTh1	ETTh2	ETTm1	ETTm2
Dataset Size	52696	17544	7207	26304	966	17420	17420	69680	69680
Variable Number	21	862	8	321	7	7	7	7	7
Sampling Frequency	10 mins	1 hour	1 day	1 hour	1 week	1 hour	1 hour	15 mins	15 mins

853  
 854      **B.2 SHORT-TERM FORECAST DATASETS**  
 855

856      The M4 dataset, which includes 100,000 heterogeneous time series from various domains, poses  
 857      a unique challenge for short-term forecasting. This is attributed to the diverse origins and distinct  
 858

859      <sup>1</sup><https://www.bgc-jena.mpg.de/wetter/>

860      <sup>2</sup><https://pems.dot.ca.gov/>

861      <sup>3</sup><https://archive.ics.uci.edu/dataset/321/electricityloaddiagrams20112014>

862      <sup>4</sup><https://github.com/laiguokun/multivariate-time-series-data>

863      <sup>5</sup><https://github.com/laiguokun/multivariate-time-series-data>

864      <sup>6</sup><https://github.com/zhouhaoyi/ETDataset>

864 temporal characteristics of the data, which contrast with the uniformity typically found in long-term  
 865 forecasting datasets. A statistical overview of the dataset is provided in Table 8.  
 866

867 Table 8: Dataset descriptions of M4 forecasting  
 868

Dataset	Sample Numbers (train set, test set)	Variable Number	Prediction Length
M4 Yearly	(23000, 23000)	1	6
M4 Quarterly	(24000, 24000)	1	8
M4 Monthly	(48000, 48000)	1	18
M4 Weekly	(359, 359)	1	13
M4 Daily	(4227, 4227)	1	14
M4 Hourly	(414, 414)	1	48

875  
 876 B.3 CLASSIFICATION DATASETS  
 877

878 The UEA dataset comprises a diverse collection of time series samples across various domains,  
 879 designed for classification tasks. It encompasses a broad spectrum of recognition tasks, including  
 880 facial, gesture, and action recognition, as well as audio identification. Furthermore, it extends its  
 881 utility to practical applications in industrial monitoring, health surveillance, and medical diagnostics,  
 882 with a particular emphasis on the analysis of cardiac data. Typically, the dataset is organized into  
 883 10 distinct classes. Table 9 offers a detailed overview of the classification statistics for the UEA  
 884 datasets, underscoring their extensive applicability across multiple domains.

885 Table 9: Datasets and mapping details of UEA dataset  
 886

Dataset	Sample Numbers (train set, test set)	Variable Number	Series Length
EthanolConcentration	(261, 263)	3	1751
FaceDetection	(5890, 3524)	144	62
Handwriting	(150, 850)	3	152
Heartbeat	(204, 205)	61	405
JapaneseVowels	(270, 370)	12	29
PEMS - SF	(267, 173)	963	144
SelfRegulationSCP1	(268, 293)	6	896
SelfRegulationSCP2	(200, 180)	7	1152
SpokenArabicDigits	(6599, 2199)	13	93
UWaveGestureLibrary	(120, 320)	3	315

897 B.4 ANOMALY DETECTION DATASETS  
 898

899 Our benchmarking process utilizes datasets that cover a range of domains, such as server machinery,  
 900 spacecraft, and infrastructure systems. These datasets are carefully organized into three distinct  
 901 phases: training, validation, and testing. Each dataset consists of a single, continuous time series,  
 902 and samples are extracted using a uniform, fixed-length sliding window method. Table 10 presents  
 903 a comprehensive statistical summary of these datasets, illustrating their structured arrangement and  
 904 the systematic approach to sample extraction.

905 B.5 DATASET VISUALIZATION  
 906

907 908 Figure 9,10,11 and 12 shows the pairwise correlation among the variables in ETT dataset.  
 909  
 910  
 911  
 912  
 913  
 914  
 915  
 916  
 917

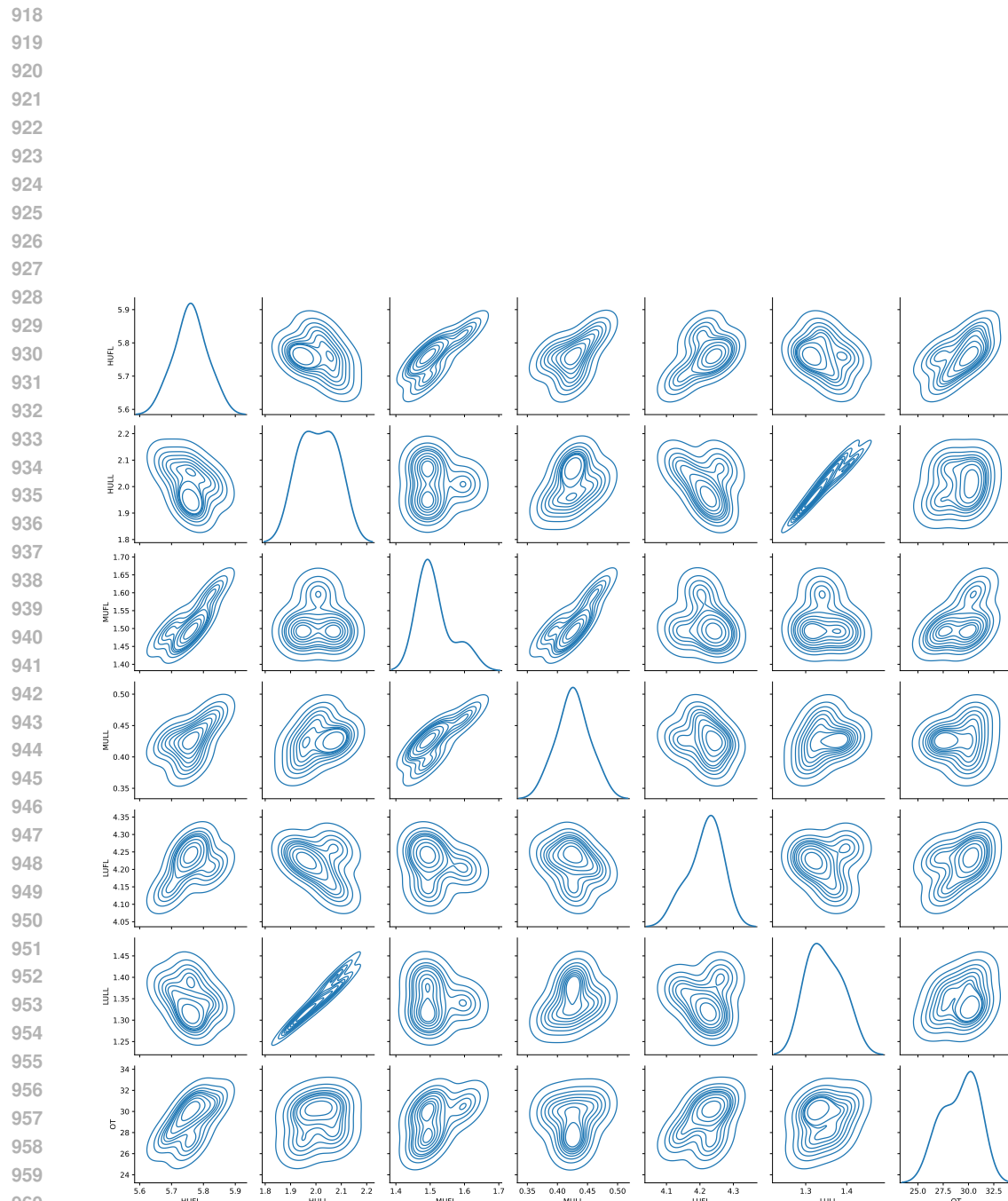


Figure 9: Pairwise correlation among the variables(ETTm1).

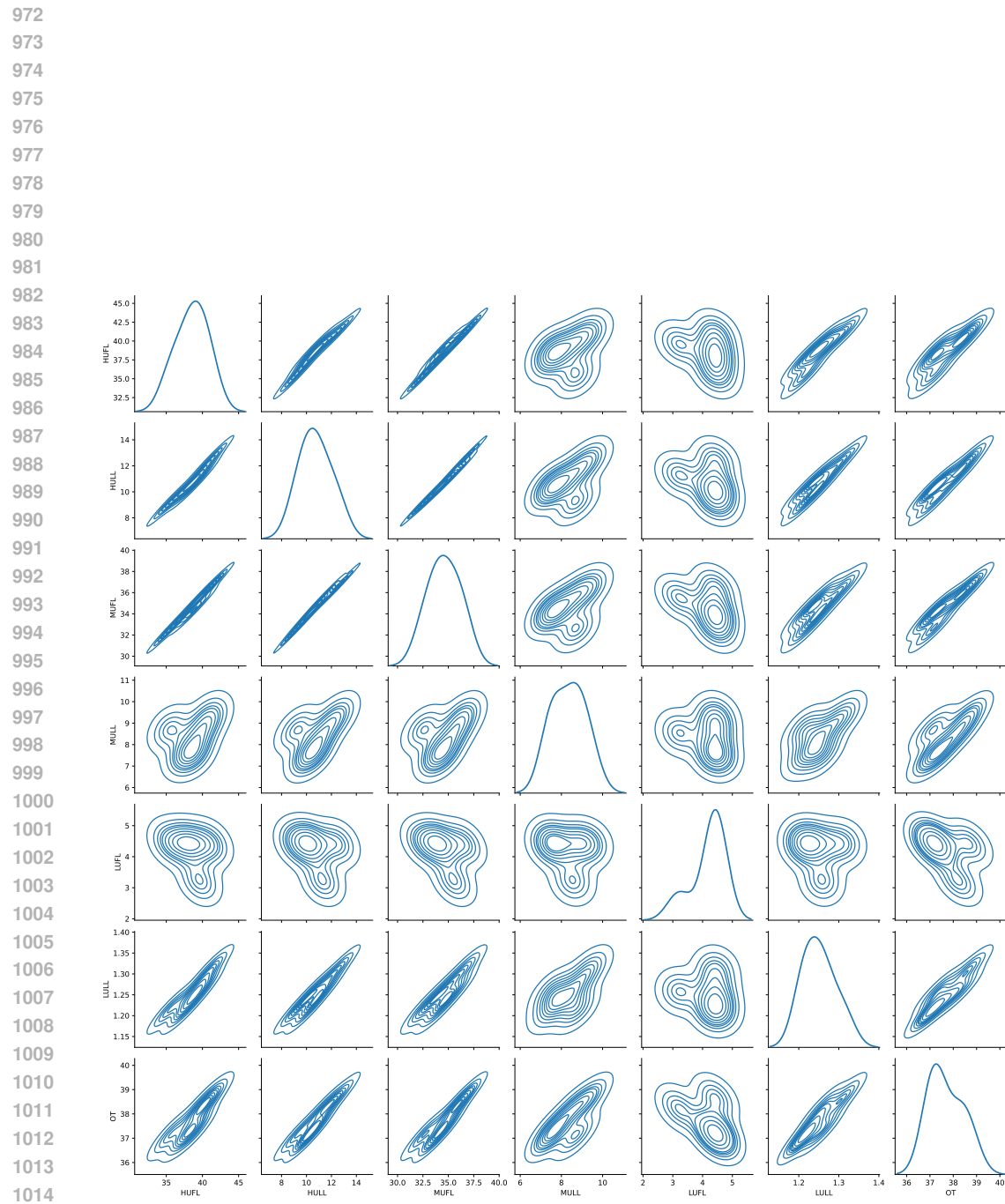


Figure 10: Pairwise correlation among the variables(ETTm2).

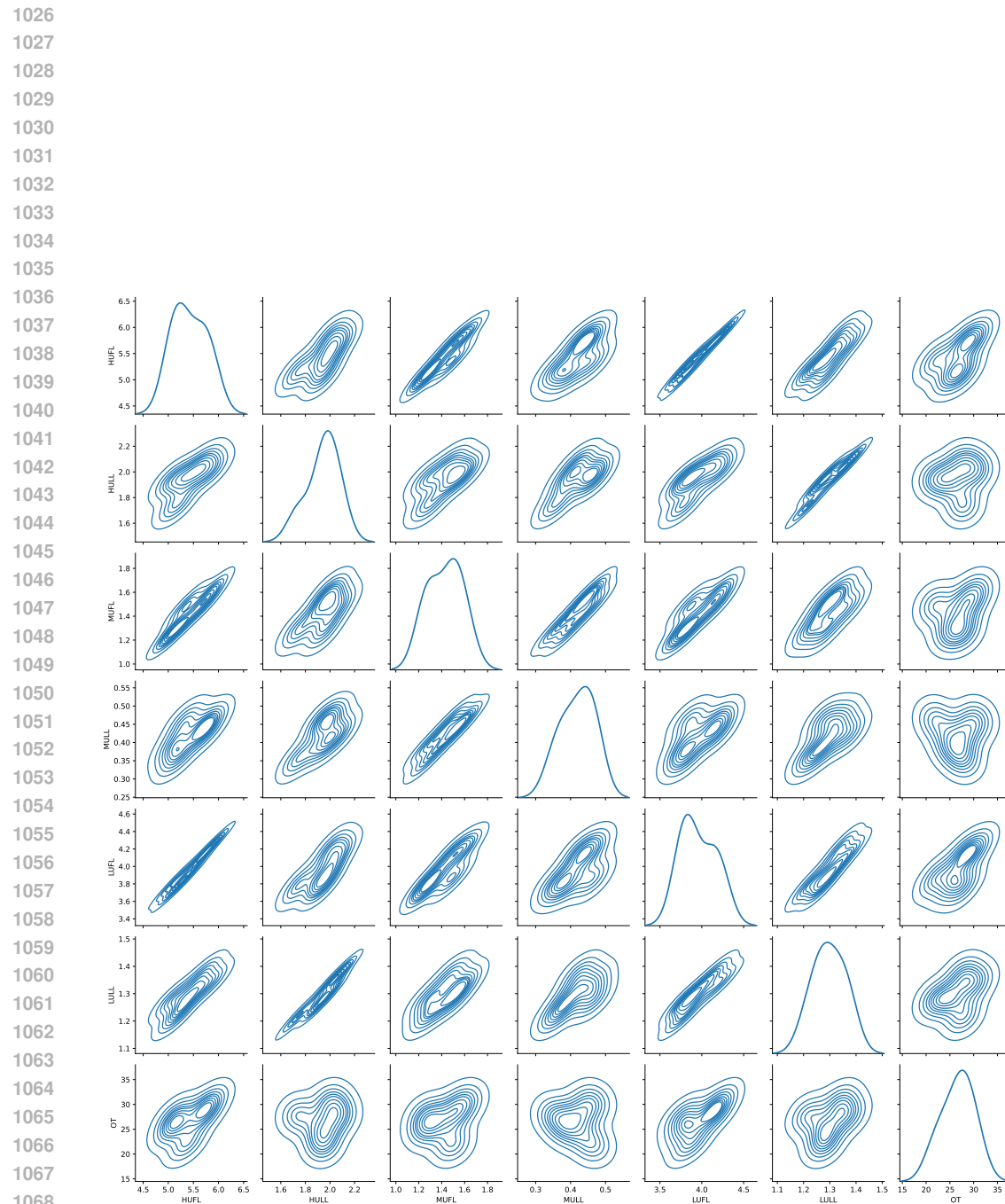


Figure 11: Pairwise correlation among the variables(ETTh1).

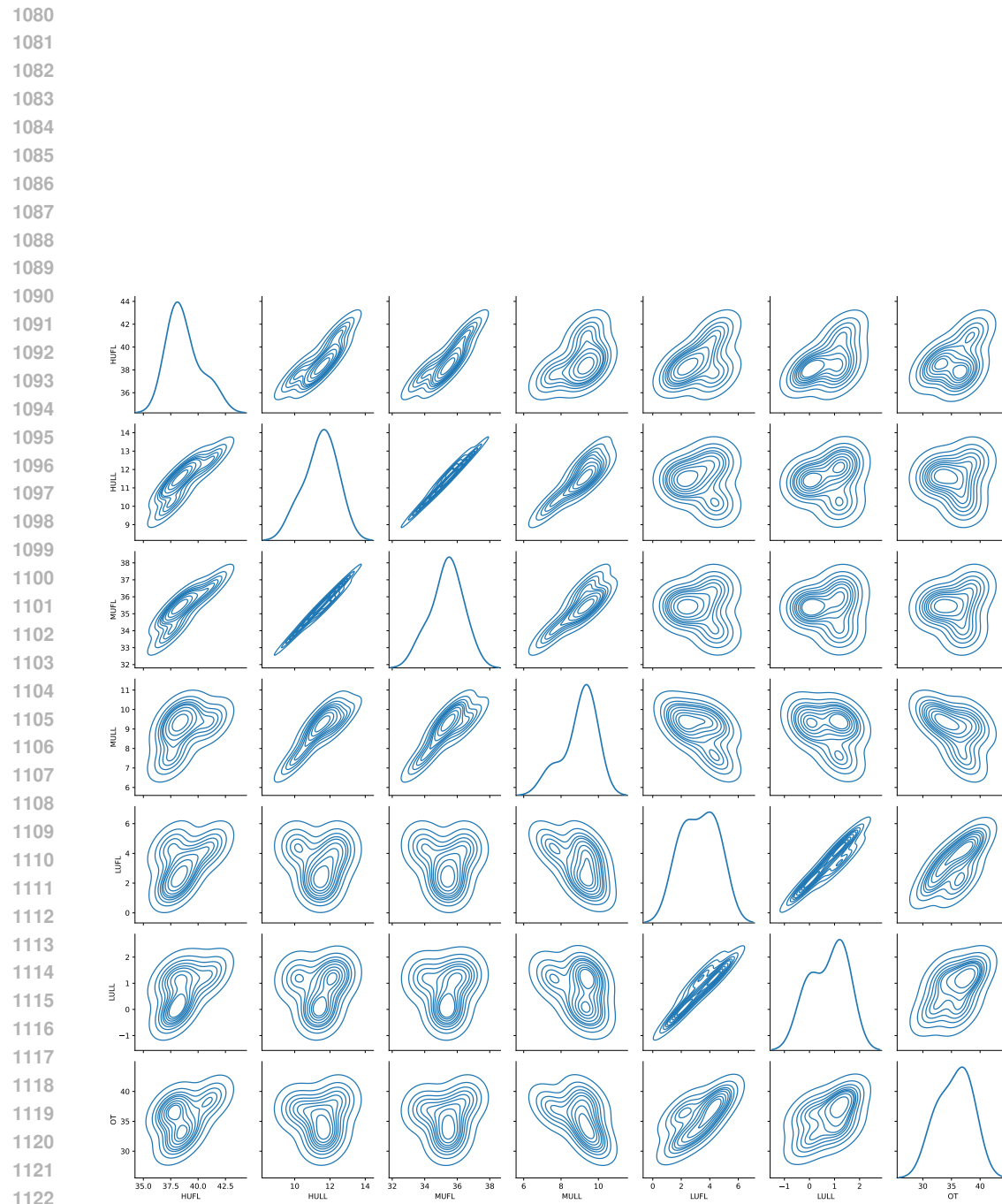


Figure 12: Pairwise correlation among the variables(ETTh2).

Table 10: Dataset sizes and details for anomaly detection datasets

Dataset	Dataset sizes (train set, val set, test set)	Variable Number	Sliding Window Length
SMD	(566724, 141681, 708420)	38	100
MSL	(44653, 11664, 73729)	55	100
SMAP	(108146, 27037, 427617)	25	100
SWaT	(396000, 99000, 449919)	51	100
PSM	(105984, 26497, 87841)	25	100

## C EXPERIMENT DETAILS

Table 11: Model Hyper-parameters and Training Process for Different Tasks/Configurations(TVNet)

Tasks/Configurations	Model Hyper-parameter				Training Process			
	$k$ (kernel size)	Layers	$C_m$	$P$ (Patch length)	LR	Loss	Batch Size	Epochs
Long-term Forecasting	3x3	3	64	24	$10^{-4}$	MSE	32	10
Short-term Forecasting	3x3	3	64	8	$10^{-3}$	SMAPE	16	10
Imputation	3x3	3	64	1	$10^{-3}$	MSE	16	10
Classification	3x3	3	Eq31	1	$10^{-3}$	Cross Entropy	16	30
Anomaly Detection	3x3	5	Eq32	8	$10^{-4}$	MSE	128	10

- LR refers to the learning rate, and we have incorporated an early stopping mechanism to enhance the training process. For long-term forecasting task, Input lenght is set to 96Wu et al. (2022a).
- We performed experiments using 5 distinct random seeds: 1111, 333, 2023, 2024, and 2025.

### C.1 LONG-TERM FORECASTING

**Implementation details:** Our method utilizes the mean squared error (MSE) loss function and is optimized using the ADAM optimizer (Kingma, 2014), with an initial learning rate set to  $10^{-4}$ . The training regimen consists of 10 epochs, augmented by an appropriate early stopping mechanism. We employ the mean squared error (MSE) and mean absolute error (MAE) as evaluation metrics. The deep learning models are implemented using PyTorch (Paszke et al., 2019) and executed on NVIDIA RTX4090 GPU.

**Model parameter:** TVNet comprises 3 3D-blocks, with the embedding dimensions ( $C_m$ ) set to 64. The patch length ( $P$ ) is established at 24, and the kernel size ( $k$ ) for 2D convolutions is  $3 \times 3$ . The random seed is set to 2024.

**Metrics:** The mean square error (MSE) and mean absolute error (MAE) are adopted for long-term forecasting.

$$MSE = \frac{1}{T} \sum_{i=0}^T (\hat{x}_i - x_i)^2 \quad (26)$$

$$MAE = \frac{1}{T} \sum_{i=0}^T |\hat{x}_i - x_i| \quad (27)$$

where  $T$  is the number of observations,  $\hat{x}_i$  is the predicted value, and  $x_i$  is the actual value for observation  $i$ .

### C.2 SHORT-TERM FORECASTING

**Implementation details:** Our method employs the Symmetric Mean Absolute Percentage Error (SMAPE) loss function and is optimized using the ADAM optimizer (Kingma, 2014), with an initial

learning rate of  $10^{-3}$ . The training regimen consists of 10 epochs, augmented by an appropriate early stopping mechanism. We utilize the SMAPE, Mean Absolute Scaled Error (MASE), and Overall Weighted Average (OWA) as evaluation metrics.

**Model parameter:** TVNet consists of 3 3D-blocks, with the embedding dimension  $C_m$  configured to 64. The patch length  $P$  is set to 8, and the kernel size  $k$  for 2D convolutions is  $3 \times 3$ . The random seed is set to 2024.

**Metrics:** For short-term forecasting, in accordance with (Wu et al., 2022a), we utilize the Symmetric Mean Absolute Percentage Error (SMAPE), Mean Absolute Scaled Error (MASE), and Overall Weighted Average (OWA) as the metrics. These metrics can be computed as follows:

$$\text{SMAPE} = \frac{200}{T} \sum_{i=1}^T \frac{|x_i - \hat{x}_i|}{|x_i| + |\hat{x}_i|} \quad (28)$$

$$\text{MASE} = \frac{1}{T} \sum_{i=1}^T \frac{|x_i - \hat{x}_i|}{\frac{1}{T-p} \sum_{j=p+1}^T |x_j - x_{j-p}|} \quad (29)$$

$$\text{OWA} = \frac{1}{2} \left[ \frac{\text{SMAPE}}{\text{SMAPE}_{\text{Naive2}}} + \frac{\text{MASE}}{\text{MASE}_{\text{Naive2}}} \right] \quad (30)$$

where  $p$  is the periodicity of data,  $T$  is the number of observations,  $\hat{x}_i$  is the predicted value, and  $x_i$  is the actual value for observation  $i$ .

### C.3 IMPUTATION

**Implementation details:** Our method utilizes the mean squared error (MSE) loss function and is optimized using the ADAM optimizer (Kingma, 2014), with an initial learning rate set to  $10^{-3}$ . The training regimen consists of 10 epochs, augmented by an appropriate early stopping mechanism. We employ the mean squared error (MSE) and mean absolute error (MAE) as evaluation metrics.

**Model parameter:** TVNet has 3 blocks. The patch length  $P$  is set to 1 to avoid mixing the masked and unmasked tokens, with the embedding dimension  $C_m$  configured to 64. The random seed is set to 2024

### C.4 CLASSIFICATION

**Implementation details:** Our method employs the Cross-Entropy Loss and is optimized using the ADAM optimizer, initialized with a learning rate of  $10^{-3}$ . The training regimen consists of 30 epochs, complemented by an appropriate early stopping mechanism. Classification accuracy serves as the metric for evaluation.

**Model parameter:** By default, TVNet comprises three blocks. The equation determines the channel number  $C_m$ . The random seed is set to 2024.

$$C_m = \min \left\{ \max \left( 2^{\lfloor \log_2 M \rfloor}, d_{\min} \right), d_{\max} \right\} \quad (31)$$

where  $d_{\min}$  is 32 and  $d_{\max}$  is 64, in accordance with the predefined criteria. The patch length  $P$  is established at 1.

**Metrics:** For classification, the accuracy is calculated as the metric.

### C.5 ANOMALY DETECTION

**Implementation details:** In the classical reconstruction task, we employ MSE loss for training. The ADAM optimizer is utilized, initialized with a learning rate of  $\times 10^{-4}$ . The training regimen consists of 10 epochs, complemented by an appropriate early stopping mechanism. The reconstruction error, quantified as the Mean Squared Error (MSE), serves as the criterion for anomaly detection. The F1-Score is adopted as the metric.

1242 **Model parameter:** By default, TVNet comprises 3 blocks. The channel number  $C_m$  is determined  
 1243 by the equation

$$C_m = \min \left\{ \max \left( 2^{\lfloor \log_2 M \rfloor}, d_{\min} \right), d_{\max} \right\} \quad (32)$$

1244 where  $d_{\min}$  is 32 and  $d_{\max}$  is 128, in accordance with the predefined criteria. The patch length  $P$  is  
 1245 established at 8.

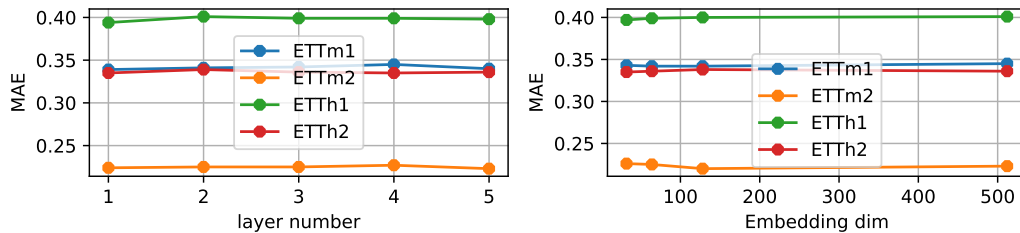
1246 **Metrics:** For anomaly detection, we adopt the F1-score, which is the harmonic mean of precision  
 1247 and recall.

## D HYPERPARAMETER SENSITIVITY

### D.1 MODEL HYPERPARAMETERS

In this section, we assess the robustness of TVNet by examining its sensitivity to model hyperparameters. We will meticulously assess the impact of hyperparameter tuning on long-term forecasting models, focusing on the embedding dimensions( $C_m$ ), the number of blocks, and the patch length( $P$ ) and kernel size( $k$ ) to enhance the accuracy of our predictions.

**Embedding Dimensions and Number of blocks:** Figure 13 shows the different effect about DataEmbedding dimension( $C_m = 32, 64, 128, 512$ ) and the number of 3D-blocks(1, 2, 3, 4, 5) on ETT datasets(Prediction length = 96).Table 12 shows the effects of different  $C_m$  on the three data sets(ETTh1, Weather and Electricity) for long-term prediction tasks of different prediction lengths.According to the above results, the model shows better robustness for DataEmbedding Dimension  $C_m$ and the number of 3D-Blocks.



1274 Figure 13: Hyperparameter sensitivity concerning the dimension of DataEmbedding and number of  
 1275 blocks

1276 Table 12: Impact of different DataEmbedding dimension. A lower MSE or MAE indicates a better  
 1277 performance.

Models	Metrics	ETTh1				Weather				Electricity			
		96	192	336	720	96	192	336	720	96	192	336	720
$C_m = 32$	MSE	0.369	0.399	0.403	0.460	0.149	0.192	0.235	0.306	0.139	0.168	0.162	0.189
$C_m = 32$	MAE	0.407	0.409	0.414	0.457	0.195	0.237	0.281	0.336	0.228	0.246	0.265	0.287
$C_m = 64$	MSE	0.371	0.398	0.401	0.458	0.147	0.194	0.235	0.308	0.142	0.165	0.164	0.190
$C_m = 64$	MAE	0.408	0.409	0.409	0.459	0.198	0.238	0.277	0.331	0.223	0.241	0.269	0.284
$C_m = 128$	MSE	0.365	0.389	0.395	0.451	0.153	0.187	0.240	0.306	0.140	0.157	0.166	0.182
$C_m = 128$	MAE	0.404	0.403	0.406	0.453	0.196	0.235	0.276	0.329	0.219	0.238	0.270	0.285

1287 **Patch length and Kernel size:** In this section, we conducted experiments on long-term forecasting  
 1288 tasks by varying the Patch length ( $P$ ) and Kernel size ( $k$ ). We tested four distinct values for Patch  
 1289 length (8, 12, 24, 32). To maintain the dimensionality of each feature map layer, we employed zero-  
 1290 padding equivalent to (kernel size - 1). The results presented in Table 14 indicate that both  
 1291 extremely small and large convolution kernels negatively impact the prediction accuracy. This study  
 1292 advocates for the adoption of a  $3 \times 3$  convolution kernel, which strikes a balance between capturing  
 1293 local features and maintaining computational efficiency. For the Patch length ( $P$ ), our findings indicate  
 1294 that both smaller and larger values can degrade the forecasting performance. In the context of  
 1295 long-term forecasting, we recommend setting the Patch length to 24, as it offers an optimal balance  
 1296 for prediction accuracy.

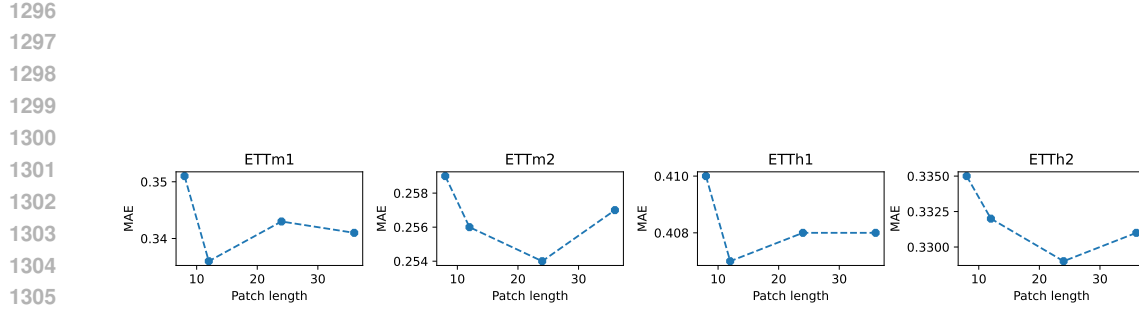


Figure 14: Hyperparameter sensitivity concerning patch length(prediction length=96)

Table 13: Impact of different Patch length.A lower MSE or MAE indicates a better performance.

Models	Metrics	ETTh1				Weather				Electricity			
		96	192	336	720	96	192	336	720	96	192	336	720
$P = 8$	MSE	0.384	0.406	0.404	0.463	0.153	0.197	0.236	0.309	0.147	0.163	0.172	0.193
	MAE	0.413	0.417	0.412	0.463	0.204	0.251	0.286	0.334	0.226	0.247	0.272	0.289
$P = 12$	MSE	0.369	0.404	0.402	0.449	0.153	0.205	0.237	0.311	0.146	0.170	0.163	0.191
	MAE	0.406	0.411	0.412	0.463	0.209	0.245	0.287	0.332	0.227	0.246	0.265	0.280
$P = 24$	MSE	0.371	0.398	0.401	0.458	0.147	0.194	0.235	0.308	0.142	0.165	0.164	0.190
	MAE	0.408	0.409	0.409	0.459	0.198	0.238	0.277	0.331	0.223	0.241	0.269	0.284
$P = 32$	MSE	0.368	0.395	0.399	0.454	0.150	0.192	0.241	0.311	0.145	0.167	0.155	0.192
	MAE	0.401	0.407	0.420	0.457	0.205	0.239	0.277	0.332	0.227	0.242	0.252	0.288

Table 14: Impact of different kernel sizes. A lower MSE or MAE indicates a better performance.

Models	Metrics	ETTh1				ETTm1				Electricity			
		96	192	336	720	96	192	336	720	96	192	336	720
$k = 1$	MSE	0.375	0.407	0.405	0.464	0.293	0.327	0.371	0.412	0.143	0.171	0.169	0.196
	MAE	0.413	0.417	0.415	0.464	0.358	0.371	0.392	0.419	0.221	0.249	0.265	0.302
$k = 3$	MSE	0.371	0.398	0.401	0.458	0.288	0.326	0.365	0.412	0.142	0.165	0.164	0.190
	MAE	0.408	0.409	0.409	0.459	0.343	0.367	0.391	0.413	0.223	0.241	0.269	0.284
$k = 5$	MSE	0.369	0.396	0.399	0.454	0.289	0.324	0.367	0.417	0.146	0.168	0.165	0.187
	MAE	0.405	0.408	0.409	0.457	0.339	0.362	0.390	0.415	0.220	0.240	0.264	0.279
$k = 7$	MSE	0.370	0.399	0.398	0.450	0.291	0.325	0.368	0.420	0.147	0.167	0.164	0.189
	MAE	0.406	0.409	0.409	0.462	0.341	0.360	0.391	0.426	0.225	0.239	0.267	0.281
$k = 9$	MSE	0.386	0.413	0.407	0.474	0.302	0.349	0.403	0.419	0.157	0.189	0.194	0.212
	MAE	0.437	0.444	0.439	0.485	0.372	0.396	0.410	0.432	0.230	0.271	0.285	0.314

1350  
1351

## D.2 TRAINING PROCESS

1352  
1353  
1354  
1355  
1356  
1357

Furthermore, acknowledging that hyperparameters such as learning rate and batch size influence the results, we present experimental results inclusive of standard deviation. We explore batch sizes ranging from 32 to 512, learning rates from  $10^{-5}$  to 0.05, five seeds(1111,333,2023,2024,2025), and training epochs from 10 to 100. The findings are summarized in Table 15 and Table 16 for long-term forecasting and short-term forecasting. The results show that TVNet has high robustness for different training process parameter selection

1358  
1359  
1360  
1361

Table 15: Detailed performance of TVNet. We report MSE/MAE and standard deviation of different forecasting horizons {24, 36, 48, 60} for ILI and {96, 192, 336, 720} for others.  $H_1, H_2, H_3, H_4$  means the horizons.

1362  
1363  
1364  
1365  
1366  
1367  
1368  
1369  
1370  
1371  
1372

Horizon	Electricity			ETTh2			Exchange		
	MSE	MAE		MSE	MAE		MSE	MAE	
$H_1$	$0.142 \pm 0.002$	$0.223 \pm 0.003$		$0.263 \pm 0.003$	$0.329 \pm 0.003$		$0.080 \pm 0.002$	$0.195 \pm 0.003$	
$H_2$	$0.165 \pm 0.002$	$0.241 \pm 0.006$		$0.319 \pm 0.003$	$0.372 \pm 0.002$		$0.163 \pm 0.004$	$0.285 \pm 0.002$	
$H_3$	$0.164 \pm 0.003$	$0.269 \pm 0.002$		$0.311 \pm 0.004$	$0.373 \pm 0.002$		$0.291 \pm 0.003$	$0.394 \pm 0.003$	
$H_4$	$0.190 \pm 0.005$	$0.284 \pm 0.002$		$0.401 \pm 0.003$	$0.434 \pm 0.004$		$0.658 \pm 0.007$	$0.594 \pm 0.002$	
Horizon	ILI			Traffic			Weather		
	MSE	MAE		MSE	MAE		MSE	MAE	
$H_1$	$1.324 \pm 0.006$	$0.712 \pm 0.004$		$0.367 \pm 0.003$	$0.252 \pm 0.003$		$0.147 \pm 0.005$	$0.198 \pm 0.004$	
$H_2$	$1.190 \pm 0.020$	$0.772 \pm 0.018$		$0.381 \pm 0.003$	$0.262 \pm 0.004$		$0.194 \pm 0.003$	$0.238 \pm 0.003$	
$H_3$	$1.456 \pm 0.015$	$0.782 \pm 0.004$		$0.395 \pm 0.004$	$0.268 \pm 0.003$		$0.235 \pm 0.005$	$0.277 \pm 0.005$	
$H_4$	$1.652 \pm 0.022$	$0.796 \pm 0.005$		$0.442 \pm 0.004$	$0.290 \pm 0.006$		$0.308 \pm 0.003$	$0.331 \pm 0.003$	

1373

Table 16: Detailed performance of TVNet. We report standard deviation on short-term forecasting

1374  
1375  
1376  
1377

## E MORE ABLATION EXPERIMENTS

1380  
1381  
1382

## E.1 INTER-POOL MODULE

1383  
1384  
1385

In this section, we further conducted ablation studies on the tasks of short-term forecasting and time series anomaly detection, and presented the results.(Table 19)

1386  
1387

Table 17: Ablation of Inter-pool Module.(Anomaly detection(F1) and Short-term forecasting(OWA))

1388  
1389  
1390  
1391  
1392  
1393

Dataset	Model	SMD	MSL	SMAP	SWaT	PSM
Anomaly Detection	<b>Ours</b>	85.75	85.16	71.64	93.72	97.53
	w/o	78.61	67.34	59.82	82.74	86.27
Dataset	Model	Yearly	Quarterly	Monthly	Others	
Short-term forecasting	<b>Ours</b>	0.768	0.876	0.866	0.969	
	w/o	0.809	1.231	0.929	1.205	

1394  
1395  
1396

## E.2 RESHAPE REPRESENTATION

1397  
1398  
1399  
1400  
1401  
1402  
1403

The existing representations for time series include 1D, 2D (inter-pool, cross-dimensions), and 3D (inter-pool, intra-pool, and cross-dimensions). To demonstrate the effectiveness of the 3D-embedding(③) proposed in this paper, 1D-embedding  $X_{emb} \in \mathcal{R}^{L \times C_m}$  (label ①) and 2D-embedding  $X_{emb} \in \mathcal{R}^{N \times P \times C_m}$  (label ②) are designed following the same rationale. For the time series analysis task using **fixed weight convolution** for different methods, long-term forecasting(Prediction length =192) is tested. Table 18 shows the result. It can be seen from the results that the error is smaller than that of 1D-Embedding and 2D-Embedding. 3D-Embedding, indicating that 3D-Embedding can better represent time series.

Table 18: Different Embedding ways for long-term forecasting.

Embedding	Electricity		ETTh2		Exchange	
	MSE	MAE	MSE	MAE	MSE	MAE
①	0.214	0.318	0.347	0.391	0.185	0.320
②	0.209	0.304	0.333	0.386	0.171	0.312
③	<b>0.201</b>	<b>0.296</b>	<b>0.330</b>	<b>0.381</b>	<b>0.164</b>	<b>0.296</b>
Embedding	ETTm1		Traffic		Weather	
	MSE	MAE	MSE	MAE	MSE	MAE
①	0.357	0.392	0.440	0.349	0.271	0.292
②	0.332	0.383	0.427	0.320	0.262	0.271
③	<b>0.336</b>	<b>0.385</b>	<b>0.423</b>	<b>0.313</b>	<b>0.257</b>	<b>0.269</b>

Table 19: Different Embedding ways for Anomaly-detection and short-term forecasting.

Dataset	Model	SMD	MSL	SMAP	SWaT	PSM
Anomaly Detection	①	67.38	70.29	65.43	75.41	85.77
	②	70.60	65.95	52.09	76.54	82.05
	③	80.21	83.24	69.41	87.65	92.34
Dataset	Model	Yearly	Quarterly	Monthly	Others	
Short-term forecasting	①	1.043	1.576	1.132	1.574	
	②	0.904	1.589	1.076	1.322	
	③	0.839	1.375	1.034	1.323	

### E.3 TRAINING SPEED AND MEMORY

Considering that the hyperparameters set during different training processes and the look-back window can affect the number of model parameters and running speed, to make a fairer comparison of the parameters and training speed of different models, we selected three typical models: PatchTST (Transformer-based), Dlinear (MLP-based), and ModernTCN (CNN-based), as well as the model proposed in this paper for comparison. We unified the training hyperparameters as shown in Table 11. The results for different input lengths on ETTm2 (prediction length fixed at 96) are shown in Figure 15. From the figure, it can be observed that in terms of running speed, as the input length increases, the training time of PatchTST increases, and the memory usage of ModernTCN increases significantly. In contrast, the training time and memory usage of the TVNet proposed in this paper increase slowly with the increase of input length, proving the superiority of the proposed model in terms of efficiency and effectiveness.

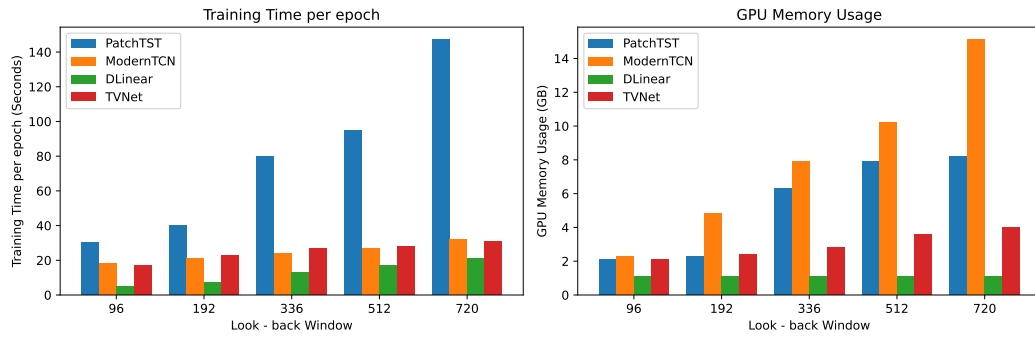


Figure 15: Params and GPU Memory for different input length(ETTm2)

### F MORE EXTRA EXPERIMENTS STUDIES

We have conducted additional experiments and analyses.

1458  
1459

## F.1 INPUT LENGTH

1460  
1461  
1462  
1463  
1464  
1465  
1466  
1467

**Impact of input length:** In time series forecasting, the input length dictates the extent of historical data available for the algorithm’s analysis. Typically, models that excel at capturing long-term dependencies tend to exhibit superior performance with increasing input lengths. To substantiate this, we evaluated our model across a range of input lengths while maintaining constant prediction lengths. Figure 16 illustrates that the performance of transformer-based models diminishes with longer inputs due to the prevalence of repetitive short-term patterns. Conversely, TVNet’s predictive accuracy consistently improves with extended input lengths, suggesting its proficiency in capturing long-term dependencies and extracting meaningful information effectively.

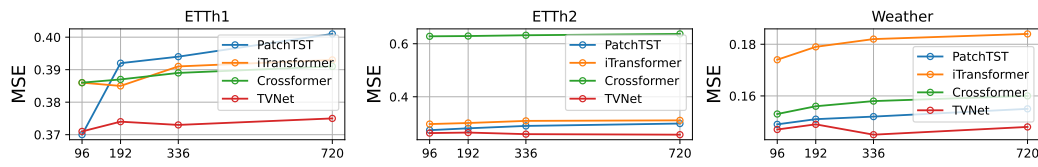
1468  
1469  
1470  
1471  
1472  
14731474  
1475  
1476  
1477

Figure 16: The MSE results with different input lengths and same prediction lengths(ETTh1,ETTh2 and Weather) prediction length( $L$ )=192

1478  
1479  
1480  
1481  
1482  
1483  
1484  
1485  
1486  
1487

## F.2 MODEL ROBUSTNESS

We employ a straightforward noise injection technique to ascertain the robustness of our model. Specifically, we randomly select a proportion  $\epsilon$  of data from the original input sequence and introduce random perturbations within the range  $[-2X_i, 2X_i]$ , where  $X_i$  represents the original data values. The perturbed data is subsequently utilized for training, and the mean squared error (MSE) and mean absolute error (MAE) metrics are documented. The findings are presented in Table 20. An increase in the perturbation ratio  $\epsilon$  leads to a marginal rise in both MSE and MAE, indicating that TVNet demonstrates commendable robustness against mild noise (up to 10%) and excels at handling significant data anomalies, such as those caused by equipment malfunctions in power data.

1488  
1489  
1490  
1491  
1492  
1493  
1494  
1495  
1496  
1497  
1498

Table 20: Different  $\epsilon$  indicates different proportions of noise injection.

Models	Metrics	Weather				Electricity				Traffic			
		96	192	336	720	96	192	336	720	96	192	336	720
TVNet	MSE	0.147	0.194	0.235	0.308	0.142	0.165	0.164	0.190	0.367	0.381	0.395	0.442
	MAE	0.198	0.238	0.277	0.331	0.223	0.241	0.269	0.284	0.252	0.262	0.268	0.290
$\epsilon = 1\%$	MSE	0.146	0.192	0.238	0.305	0.142	0.165	0.167	0.191	0.365	0.382	0.396	0.444
	MAE	0.197	0.236	0.280	0.332	0.225	0.244	0.271	0.286	0.255	0.260	0.267	0.292
$\epsilon = 5\%$	MSE	0.150	0.196	0.238	0.307	0.148	0.170	0.166	0.191	0.369	0.380	0.399	0.445
	MAE	0.195	0.239	0.281	0.335	0.227	0.248	0.271	0.283	0.257	0.260	0.273	0.290
$\epsilon = 10\%$	MSE	0.159	0.207	0.245	0.310	0.149	0.176	0.177	0.194	0.379	0.386	0.405	0.451
	MAE	0.205	0.247	0.289	0.336	0.229	0.245	0.279	0.283	0.265	0.271	0.278	0.294

1499  
1500  
1501  
1502  
1503  
1504  
1505  
1506  
1507  
1508  
1509  
1510  
1511

## F.3 UNIVARIATE LONG-TERM FORECASTING RESULTS

Table 21 shows the Univariate long-term forecasting results.

1512  
 1513  
 1514  
 1515  
 1516  
 1517  
 1518  
 1519  
 1520  
 1521  
 1522  
 1523  
 1524  
 1525  
 1526  
 1527  
 1528  
 1529  
 1530

1531 Table 21: Following PatchTS(Nie et al., 2022) input length is fixed as 336 and prediction lengths  
 1532 are  $T \in \{96, 192, 336, 720\}$ . The best results are in **bold**.

1533

Models	Metrics	TVNet		PatchTST		DLinear		FEDformer		Autoformer		Informer		LogTrans	
		MSE	MAE	MSE	MAE	MSE	MAE	MSE	MAE	MSE	MAE	MSE	MAE	MSE	MAE
ETTh1	96	<b>0.053</b>	<b>0.179</b>	0.055	0.179	0.056	0.180	0.079	0.215	0.071	0.206	0.193	<b>0.377</b>	0.283	0.468
	192	<b>0.067</b>	<b>0.202</b>	0.071	0.205	0.071	0.204	0.104	0.245	0.114	0.262	0.217	<b>0.295</b>	0.234	0.409
	336	<b>0.071</b>	<b>0.210</b>	0.076	0.220	0.098	0.244	0.119	0.270	0.107	0.258	0.202	<b>0.381</b>	0.286	0.546
	720	<b>0.083</b>	<b>0.229</b>	0.087	0.236	0.087	0.359	0.142	0.299	0.126	0.283	0.183	<b>0.355</b>	0.475	0.629
ETTh2	96	<b>0.121</b>	<b>0.268</b>	0.129	0.282	0.131	0.279	0.128	0.271	0.153	0.306	0.213	<b>0.373</b>	0.217	0.379
	192	<b>0.164</b>	<b>0.320</b>	0.168	0.328	0.176	0.329	0.185	0.330	0.204	0.351	0.227	<b>0.387</b>	0.281	0.429
	336	<b>0.171</b>	<b>0.333</b>	0.171	0.336	0.209	0.367	0.231	0.378	0.246	0.389	0.242	<b>0.408</b>	0.293	0.437
	720	<b>0.219</b>	<b>0.380</b>	0.223	0.380	0.276	0.426	0.278	0.420	0.268	0.409	0.291	<b>0.439</b>	0.218	0.387
ETTm1	96	<b>0.024</b>	<b>0.120</b>	0.026	0.121	0.028	0.123	0.033	0.140	0.056	0.183	0.109	<b>0.277</b>	0.218	0.387
	192	<b>0.038</b>	<b>0.150</b>	0.039	0.150	0.045	0.156	0.058	0.186	0.081	0.216	0.151	<b>0.310</b>	0.157	0.317
	336	<b>0.053</b>	<b>0.173</b>	0.053	0.173	0.061	0.182	0.084	0.231	0.076	0.218	0.427	<b>0.591</b>	0.289	0.459
	720	<b>0.072</b>	<b>0.203</b>	0.073	0.206	0.080	0.210	0.102	0.250	0.110	0.267	0.438	<b>0.586</b>	0.430	0.579
ETTm2	96	<b>0.063</b>	<b>0.183</b>	0.065	0.186	0.063	0.183	0.067	0.198	0.065	0.189	0.088	<b>0.225</b>	0.075	0.208
	192	<b>0.089</b>	<b>0.227</b>	0.093	0.231	0.092	0.227	0.102	0.245	0.118	0.256	0.132	<b>0.283</b>	0.129	0.275
	336	<b>0.119</b>	<b>0.261</b>	0.120	0.265	0.119	0.261	0.130	0.279	0.154	0.305	0.180	<b>0.336</b>	0.154	0.302
	720	<b>0.170</b>	<b>0.322</b>	0.171	0.322	0.175	0.320	0.178	0.325	0.182	0.335	0.300	<b>0.435</b>	0.160	0.321

1547  
 1548  
 1549  
 1550  
 1551  
 1552  
 1553  
 1554  
 1555  
 1556  
 1557  
 1558  
 1559  
 1560  
 1561  
 1562  
 1563  
 1564  
 1565

1566  
1567

## F.4 LLM AND MORE BASELINES

1568  
1569  
1570

For the long-term forecasting task, we have added some new Baselines (LLM-Based and TMixer). Table 22 shows the results, from which we can see that TVNet has shown good performance in most of the forecasting results.

1571  
1572  
1573  
1574

Table 22: The complete results for **long-term forecasting** are detailed (More baselines focused on LLM), demonstrating a thorough comparison among various competitive models across four distinct forecast horizons. The Avg metric indicates the average performance across these forecast horizons.

1575

Metrics	TVNet (Ours)		S2IP-LLM (2024)		TimeLLM (2023)		GPT4TS (2024)		TimeMixer (2024)		
	MSE	MAE	MSE	MAE	MSE	MAE	MSE	MAE	MSE	MAE	
ETTh1	96	<b>0.288</b>	<b>0.343</b>	<b>0.288</b>	<b>0.346</b>	0.311	0.365	0.292	0.346	0.320	0.357
	192	<b>0.326</b>	<b>0.367</b>	<b>0.323</b>	<b>0.365</b>	0.364	0.395	0.332	0.372	0.361	0.381
	336	<b>0.365</b>	<b>0.391</b>	<b>0.359</b>	<b>0.390</b>	0.369	0.398	0.366	0.394	0.390	0.404
	720	<b>0.412</b>	<b>0.413</b>	<b>0.403</b>	<b>0.418</b>	0.416	0.425	0.417	0.421	0.454	0.441
	Avg	<b>0.348</b>	<b>0.379</b>	<b>0.343</b>	<b>0.379</b>	0.365	0.395	0.388	0.403	0.381	0.395
ETTh2	96	<b>0.161</b>	<b>0.254</b>	<b>0.165</b>	<b>0.257</b>	0.170	0.262	0.173	0.262	0.175	0.258
	192	<b>0.220</b>	<b>0.293</b>	<b>0.222</b>	<b>0.299</b>	0.229	0.303	0.229	0.301	0.237	0.299
	336	<b>0.272</b>	<b>0.316</b>	<b>0.277</b>	<b>0.330</b>	0.281	0.335	0.286	0.341	0.298	0.340
	720	<b>0.349</b>	<b>0.379</b>	<b>0.363</b>	<b>0.390</b>	0.379	0.403	0.378	0.401	0.391	0.396
	Avg	<b>0.251</b>	<b>0.311</b>	<b>0.257</b>	<b>0.319</b>	0.264	0.325	0.284	0.339	0.275	0.323
ETTm1	96	<b>0.371</b>	<b>0.408</b>	<b>0.366</b>	<b>0.396</b>	0.380	0.406	0.376	0.397	0.375	0.400
	192	<b>0.398</b>	<b>0.409</b>	<b>0.401</b>	<b>0.420</b>	0.426	0.438	0.416	0.418	0.429	0.421
	336	<b>0.401</b>	<b>0.409</b>	<b>0.412</b>	<b>0.431</b>	0.437	0.451	0.442	0.433	0.484	0.458
	720	<b>0.458</b>	<b>0.459</b>	<b>0.440</b>	<b>0.458</b>	0.515	0.509	0.477	0.456	0.498	0.482
	Avg	<b>0.407</b>	<b>0.421</b>	<b>0.406</b>	<b>0.427</b>	0.439	0.451	0.465	0.455	0.447	0.440
ETTm2	96	<b>0.263</b>	<b>0.329</b>	<b>0.278</b>	<b>0.340</b>	0.306	0.362	0.285	0.342	0.289	0.341
	192	<b>0.319</b>	<b>0.372</b>	<b>0.346</b>	<b>0.385</b>	0.346	0.385	0.354	0.389	0.372	0.392
	336	<b>0.311</b>	<b>0.373</b>	<b>0.367</b>	<b>0.406</b>	0.393	0.422	0.373	0.407	0.386	0.414
	720	0.401	<b>0.434</b>	<b>0.400</b>	0.436	<b>0.397</b>	<b>0.433</b>	0.406	0.441	0.412	0.434
	Avg	<b>0.324</b>	<b>0.377</b>	<b>0.347</b>	<b>0.391</b>	0.360	0.400	0.381	0.412	0.364	0.395
Electricity	96	0.142	<b>0.223</b>	<b>0.135</b>	<b>0.230</b>	<b>0.140</b>	0.246	0.139	0.238	0.153	0.247
	192	0.165	<b>0.241</b>	<b>0.149</b>	<b>0.247</b>	<b>0.155</b>	0.253	0.153	0.251	0.166	0.256
	336	<b>0.164</b>	<b>0.269</b>	<b>0.167</b>	<b>0.266</b>	0.175	0.279	0.169	0.266	0.185	0.277
	720	<b>0.190</b>	<b>0.284</b>	<b>0.200</b>	<b>0.287</b>	0.204	0.305	0.206	0.297	0.225	0.310
	Avg	<b>0.165</b>	<b>0.254</b>	<b>0.161</b>	<b>0.257</b>	0.168	0.270	0.167	0.263	0.182	0.272
Weather	96	<b>0.147</b>	<b>0.198</b>	<b>0.145</b>	<b>0.195</b>	0.148	0.197	0.162	0.212	0.163	0.209
	192	<b>0.194</b>	<b>0.238</b>	<b>0.190</b>	<b>0.235</b>	0.194	0.246	0.204	0.248	0.208	0.250
	336	<b>0.235</b>	<b>0.277</b>	<b>0.243</b>	<b>0.280</b>	0.248	0.285	0.254	0.286	0.251	0.287
	720	<b>0.308</b>	<b>0.331</b>	<b>0.312</b>	<b>0.326</b>	0.317	0.332	0.326	0.337	0.339	0.341
	Avg	<b>0.221</b>	<b>0.261</b>	<b>0.222</b>	<b>0.259</b>	0.226	0.265	0.237	0.270	0.240	0.271
Traffic	96	<b>0.367</b>	<b>0.252</b>	<b>0.379</b>	<b>0.274</b>	0.383	0.280	0.388	0.282	0.462	0.285
	192	<b>0.381</b>	<b>0.262</b>	<b>0.397</b>	<b>0.282</b>	0.399	0.294	0.407	0.290	0.473	0.296
	336	<b>0.395</b>	<b>0.268</b>	<b>0.407</b>	<b>0.289</b>	0.411	0.306	0.412	0.294	0.498	0.296
	720	<b>0.442</b>	<b>0.290</b>	<b>0.440</b>	<b>0.301</b>	0.448	0.319	0.450	0.312	0.506	0.313
	Avg	<b>0.396</b>	<b>0.268</b>	<b>0.405</b>	<b>0.286</b>	0.440	0.301	0.414	0.294	0.484	0.297

1602

1603

## F.5 EXOGENOUS VARIABLE FORECASTING

1604  
1605  
1606  
1607  
1608  
1609

As discussed in Timexer (Wang et al., 2024), forecasting exogenous variables is crucial in various domains, including load forecasting. Our experiments on the ETT dataset also focused on predicting such variables. Figures 17 demonstrate that TVNet consistently outperforms the optimal baseline model in exogenous variable forecasting.

1610  
1611  
1612  
1613  
1614  
1615  
1616  
1617  
1618  
1619

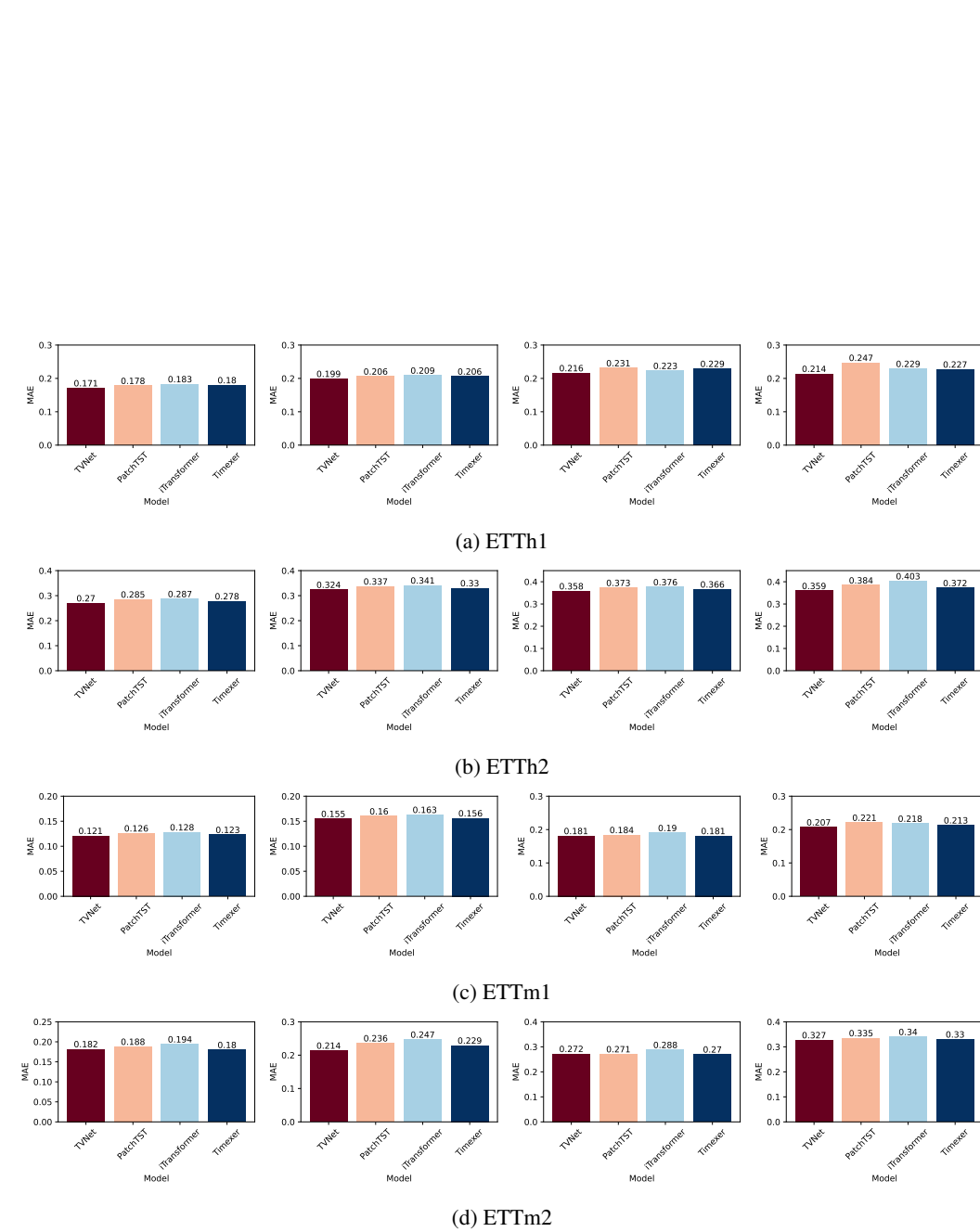


Figure 17: Exogenous variable learning results for ETT dataset.

## 1674 G FULL RESULTS

### 1675 G.1 LONG-TERM FORECASTING

1676 **Table 23:** The complete results for **long-term forecasting** are detailed, demonstrating a thorough  
 1677 comparison among various competitive models across four distinct forecast horizons. The Avg metric  
 1678 indicates the average performance across these forecast horizons.

	Models	TVNet (Ours)	PatchTST (2022)	iTransformer (2023)	Crossformer (2023)	RLinear (2023a)	MTS-Mixer (2023b)	DLinear (2023b)	TimesNet (2022a)	MICN (2023)	ModernTCN (2024)	FEDformer (2022)	RMLP (2023a)	
Metrics	MSE	MAE	MSE	MAE	MSE	MAE	MSE	MAE	MSE	MAE	MSE	MAE	MSE	MAE
ETTh1	96	<b>0.288</b> <b>0.343</b>	<b>0.290</b> <b>0.342</b>	0.334 0.368	0.316 0.373	0.301 0.342	0.314 0.358	0.299 0.343	0.338 0.375	0.314 0.360	0.292 0.346	0.326 0.390	0.298 0.345	
	192	<b>0.326</b> <b>0.367</b>	<b>0.332</b> <b>0.369</b>	0.377 0.391	0.377 0.411	0.355 0.363	0.354 0.386	0.335 0.365	0.371 0.387	0.359 0.387	<b>0.332</b> <b>0.368</b>	0.365 0.415	0.344 0.375	
	336	<b>0.365</b> <b>0.391</b>	<b>0.366</b> <b>0.392</b>	0.426 0.420	0.431 0.442	0.370 0.383	0.384 0.405	0.369 0.386	0.410 0.411	0.398 0.413	<b>0.365</b> <b>0.391</b>	0.392 0.425	0.390 0.410	
	720	<b>0.412</b> <b>0.413</b>	<b>0.416</b> 0.420	0.491 0.459	0.600 0.547	0.425 0.414	0.427 0.432	0.425 0.421	0.478 0.450	0.459 0.464	<b>0.416</b> <b>0.417</b>	0.446 0.458	0.445 0.441	
Avg		<b>0.348</b> <b>0.379</b>	<b>0.351</b> <b>0.381</b>	0.407 0.410	0.431 0.443	0.358 0.376	0.370 0.395	0.357 0.379	0.400 0.450	0.383 0.406	<b>0.351</b> <b>0.381</b>	0.382 0.422	0.369 0.393	
ETTh2	96	<b>0.161</b> <b>0.254</b>	0.165 0.255	0.180 0.264	0.421 0.461	<b>0.164</b> <b>0.253</b>	0.177 0.259	0.167 0.260	0.187 0.267	0.178 0.273	0.166 0.256	0.180 0.271	0.174 0.259	
	192	<b>0.220</b> <b>0.293</b>	0.220 0.292	0.250 0.309	0.503 0.519	<b>0.219</b> <b>0.290</b>	0.241 0.303	0.224 0.303	0.249 0.309	0.245 0.316	0.222 0.293	0.252 0.318	0.236 0.303	
	336	<b>0.272</b> <b>0.316</b>	0.274 0.329	0.311 0.348	0.611 0.580	<b>0.273</b> 0.326	0.297 0.338	0.281 0.342	<b>0.312</b> 0.351	0.295 0.350	<b>0.272</b> 0.324	0.324 0.364	0.291 0.338	
	720	<b>0.349</b> <b>0.379</b>	0.362 0.385	0.412 0.407	0.996 0.750	0.366 0.385	0.396 0.398	0.397 0.421	0.497 0.403	0.389 0.406	<b>0.351</b> <b>0.381</b>	0.410 0.420	0.371 0.391	
Avg		<b>0.251</b> <b>0.311</b>	0.255 0.315	0.288 0.332	0.632 0.578	0.256 <b>0.314</b>	0.277 0.325	0.267 0.332	0.291 0.333	0.277 0.336	<b>0.253</b> <b>0.314</b>	0.292 0.343	0.268 0.322	
ETTh3	96	0.371 0.408	<b>0.370</b> <b>0.399</b>	0.386 0.405	0.386 0.429	0.366 0.391	0.372 0.395	0.375 0.399	0.384 0.402	0.396 0.427	<b>0.368</b> <b>0.394</b>	0.376 0.415	0.390 0.410	
	192	<b>0.398</b> <b>0.409</b>	0.413 0.421	0.441 0.436	0.419 0.444	0.404 0.412	0.416 0.426	0.405 0.416	0.557 0.436	0.430 0.453	<b>0.405</b> <b>0.413</b>	0.423 0.446	0.430 0.432	
	336	<b>0.401</b> <b>0.409</b>	0.422 0.433	0.487 0.458	0.440 0.461	0.420 0.423	0.455 0.449	0.439 0.443	0.491 0.469	0.433 0.458	<b>0.391</b> <b>0.412</b>	0.444 0.462	0.441 0.441	
	720	0.458 <b>0.459</b>	<b>0.447</b> 0.466	0.503 0.491	0.519 0.524	0.442 0.456	0.475 0.472	0.472 0.490	0.521 0.500	0.474 0.508	<b>0.450</b> <b>0.461</b>	0.469 0.492	0.506 0.495	
Avg		<b>0.407</b> <b>0.421</b>	0.413 0.431	0.454 0.447	0.441 0.465	0.408 0.421	0.430 0.436	0.423 0.437	0.458 0.450	0.433 0.462	<b>0.404</b> <b>0.420</b>	0.428 0.454	0.442 0.445	
ETTh2	96	<b>0.263</b> <b>0.329</b>	0.274 0.333	0.297 0.349	0.628 0.563	<b>0.262</b> <b>0.331</b>	0.307 0.354	0.288 0.353	0.340 0.374	0.289 0.357	0.263 0.332	0.332 0.374	0.288 0.352	
	192	<b>0.319</b> <b>0.372</b>	0.339 0.379	0.380 0.400	0.703 0.624	<b>0.320</b> <b>0.374</b>	0.374 0.399	0.383 0.418	0.402 0.414	0.409 0.438	0.320 0.374	0.407 0.446	0.343 0.387	
	336	<b>0.311</b> <b>0.373</b>	0.329 0.380	0.428 0.432	0.827 0.675	0.325 0.386	0.398 0.432	0.448 0.465	0.452 0.452	0.417 0.452	<b>0.313</b> <b>0.376</b>	0.400 0.447	0.353 0.402	
	720	0.401 0.434	<b>0.379</b> <b>0.422</b>	0.427 0.445	1.181 0.840	<b>0.372</b> <b>0.421</b>	0.463 0.465	0.605 0.551	0.462 0.468	0.426 0.473	0.392 0.433	0.412 0.469	0.410 0.440	
Avg		0.324 0.377	0.330 0.379	0.383 0.407	0.835 0.676	<b>0.320</b> <b>0.378</b>	0.386 0.413	0.431 0.447	0.414 0.427	0.385 0.430	<b>0.322</b> <b>0.379</b>	0.388 0.434	0.349 0.395	
ETTh2	96	0.142 0.223	<b>0.129</b> <b>0.222</b>	0.148 0.240	0.187 0.283	0.140 0.235	0.141 0.243	0.153 0.237	0.168 0.272	0.159 0.267	<b>0.129</b> <b>0.226</b>	0.186 0.302	0.129 0.224	
	192	0.165 0.241	<b>0.147</b> <b>0.240</b>	0.162 0.253	0.258 0.330	0.154 0.248	0.163 0.261	0.152 0.249	0.184 0.289	0.168 0.279	<b>0.143</b> <b>0.239</b>	0.197 0.311	0.147 0.240	
	336	0.164 0.269	<b>0.163</b> <b>0.259</b>	0.178 0.269	0.323 0.369	0.171 0.264	0.176 0.277	0.169 0.267	0.198 0.300	0.196 0.308	<b>0.161</b> <b>0.259</b>	0.213 0.328	0.164 0.257	
	720	<b>0.190</b> <b>0.284</b>	0.197 0.290	0.225 0.317	0.404 0.423	0.209 0.297	0.212 0.308	0.233 0.344	0.220 0.320	0.203 0.312	<b>0.191</b> <b>0.286</b>	0.233 0.344	0.203 0.291	
Avg		0.165 0.254	<b>0.159</b> <b>0.253</b>	0.178 0.270	0.293 0.351	0.169 0.261	0.173 0.272	0.177 0.274	0.192 0.295	0.182 0.292	<b>0.156</b> <b>0.253</b>	0.207 0.321	0.161 <b>0.253</b>	
Weather	96	<b>0.147</b> <b>0.198</b>	<b>0.149</b> <b>0.198</b>	0.174 0.214	0.153 0.217	0.175 0.225	0.156 0.206	0.152 0.237	0.172 0.220	0.161 0.226	0.149 0.200	0.238 0.314	0.149 0.202	
	192	<b>0.194</b> <b>0.238</b>	<b>0.194</b> <b>0.241</b>	0.221 0.254	0.197 0.269	0.218 0.260	0.199 0.248	0.220 0.282	0.219 0.261	0.220 0.283	0.196 0.245	0.275 0.329	0.194 0.242	
	336	<b>0.235</b> <b>0.277</b>	0.245 0.282	0.278 0.296	0.252 0.311	0.265 0.294	0.249 0.289	0.265 0.310	0.280 0.306	0.275 0.328	<b>0.238</b> <b>0.277</b>	0.339 0.377	0.243 0.282	
	720	<b>0.308</b> <b>0.331</b>	<b>0.314</b> <b>0.333</b>	0.358 0.347	0.318 0.363	0.329 0.339	0.336 0.343	0.323 0.362	0.365 0.359	<b>0.311</b> 0.356	0.314 <b>0.334</b>	0.389 0.409	0.316 0.333	
Avg		<b>0.221</b> <b>0.261</b>	0.226 <b>0.264</b>	0.258 0.278	0.230 0.290	0.247 0.279	0.235 0.272	0.240 0.300	0.259 0.287	0.242 0.298	<b>0.224</b> <b>0.264</b>	0.310 0.357	0.225 0.265	
Traffic	96	<b>0.367</b> <b>0.252</b>	<b>0.360</b> <b>0.249</b>	0.395 0.268	0.512 0.290	0.496 0.375	0.462 0.332	0.410 0.282	0.593 0.321	0.508 0.301	0.368 0.253	0.576 0.359	0.430 0.327	
	192	<b>0.381</b> <b>0.262</b>	<b>0.379</b> <b>0.256</b>	0.417 0.276	0.522 0.297	0.503 0.377	0.488 0.354	0.423 0.287	0.617 0.336	0.536 0.315	<b>0.379</b> <b>0.261</b>	0.616 0.380	0.451 0.340	
	336	<b>0.395</b> <b>0.268</b>	<b>0.392</b> <b>0.264</b>	0.433 0.283	0.530 0.300	0.517 0.382	0.498 0.360	0.436 0.296	0.629 0.336	0.525 0.310	0.397 0.270	0.608 0.375	0.470 0.351	
	720	0.442 <b>0.290</b>	<b>0.432</b> <b>0.286</b>	0.467 0.302	0.573 0.313	0.555 0.398	0.529 0.370	0.466 0.315	0.640 0.350	0.571 0.323	<b>0.440</b> 0.296	0.621 0.375	0.513 0.372	
Avg		<b>0.396</b> <b>0.268</b>	<b>0.391</b> <b>0.264</b>	0.428 0.282	0.535 0.300	0.518 0.383	0.494 0.354	0.434 0.295	0.620 0.336	0.535 0.312	<b>0.396</b> 0.270	0.604 0.372	0.466 0.348	
Exchange	96	<b>0.080</b> <b>0.195</b>	0.093 0.214	0.086 0.206	0.186 0.346	0.083 0.301	0.083 0.020	0.081 0.203	0.107 0.234	0.102 0.235	<b>0.080</b> <b>0.196</b>	0.139 0.276	0.083 0.201	
	192	<b>0.163</b> <b>0.285</b>	0.192 0.312	0.177 0.299	0.467 0.522	0.170 0.293	0.174 0.296	<b>0.157</b> 0.293	0.226 0.344	0.172 0.316	0.166 <b>0.288</b>	0.256 0.369	0.170 0.292	
	336	<b>0.291</b> <b>0.394</b>	0.350 0.432	0.331 0.417	0.783 0.721	0.309 0.401	0.336 0.417	0.305 0.414	0.367 0.448	<b>0.272</b> 0.407	0.307 <b>0.398</b>	0.426 0.464	0.309 0.401	
	720	0.658 <b>0.594</b>	0.911 0.716	0.847 0.691	1.367 0.943	0.817 0.680	0.900 0.715	<b>0.643</b> 0.601	0.964 0.746	0.714 0.658	<b>0.656</b> <b>0.582</b>	1.090 0.800	0.816 0.680	
Avg		<b>0.298</b> <b>0.367</b>	0.387 0.419	0.360 0.403	0.701 0.633	0.345 0.394	0.373 0.407	<b>0.297</b> 0.378	0.416 0.443	0.315 0.404	0.302 <b>0.366</b>	0.478 0.478	0.345 0.394	
IL1	24	<b>1.324</b> <b>0.712</b>	<b>1.319</b> 0.754	2.207 1.032	3.040 1.186	4.337 1.507	1.472 0.798	2.215 1.081	2.317 0.934	2.684 1.112	<b>1.347</b> <b>0.717</b>	2.642 1.095	4.445 1.536	
	36	<b>1.190</b> <b>0.772</b>	1.430 0.834	1.934 0.951	3.356 1.230	4.205 1.481	1.435 0.745	1.963 0.963	1.972 0.920	2.507 1.013	1.250 0.778	2.516 1.021	4.409 1.159	
	48	<b>1.456</b> <b>0.782</b>	1.553 0.815	2.127 1.004	3.441 1.223	4.257 1.484	1.474 0.822	2.130 1.024	2.238 0.940	2.423 1.012	<b>1.388</b> <b>0.781</b>	2.505 1.041	4.388 1.507	
	60	<b>1.652</b> <b>0.796</b>	<b>1.470</b> <b>0.788</b>	2.298 0.998	3.608 1.302	4.278 1.487	1.839 0.912	2.366 1.096	2.027 0.928	2.653 1.085	1.774 0.868	2.742 1.122	4.306 1.502	
Avg</														

1728 **G.2 SHORT-TERM FORECASTING**  
 1729

1730 Table 24: The complete results for the **short-term forecasting** task in the M4 dataset are presented,  
 1731 utilizing the Weighted Average (WA) as the metric.  
 1732

	Models	TVNet (Ours)	PatchTST (2022)	U-Mixer (2024)	Crossformer (2023)	RLinear (2023a)	MTS-Mixer (2023b)	DLinear (2023)	TimesNet (2022a)	MICN (2023)	ModernTCN (2024)	FEDformer (2022)	N-HiTS (2023)
Yearly	SMAPE	<b>13.217</b>	13.258	13.317	13.392	13.944	13.548	16.965	13.387	14.935	<b>13.226</b>	13.728	13.418
	MASE	<b>2.899</b>	2.985	3.006	3.001	3.015	3.091	4.283	2.996	3.523	<b>2.957</b>	3.048	3.045
	OWA	<b>0.768</b>	0.781	0.786	0.787	0.807	0.803	1.058	0.786	0.900	<b>0.777</b>	0.803	0.793
Quarterly	SMAPE	<b>9.986</b>	10.197	9.956	16.317	10.702	10.128	12.145	10.100	11.452	<b>9.971</b>	10.792	10.202
	MASE	<b>1.159</b>	0.803	1.156	2.197	1.299	1.196	1.520	1.182	1.389	<b>1.167</b>	1.283	1.194
	OWA	<b>0.876</b>	0.803	0.873	1.542	0.959	0.896	1.106	0.890	1.026	<b>0.878</b>	0.958	0.899
Monthly	SMAPE	<b>12.493</b>	12.641	13.057	12.924	13.363	12.717	13.514	12.670	13.773	<b>12.556</b>	14.260	12.791
	MASE	<b>0.921</b>	0.930	1.067	0.966	1.014	0.931	1.037	0.933	1.076	<b>0.917</b>	1.102	0.969
	OWA	<b>0.866</b>	0.876	0.976	0.902	0.940	0.879	0.956	0.878	0.983	<b>0.866</b>	1.012	0.899
Others	SMAPE	<b>4.764</b>	4.946	4.858	5.493	5.437	4.817	6.709	4.891	6.716	<b>4.715</b>	4.954	5.061
	MASE	<b>2.986</b>	<b>2.985</b>	3.195	3.690	3.706	3.255	4.953	3.302	4.717	3.107	3.264	3.216
	OWA	<b>0.969</b>	1.044	1.015	1.160	1.157	1.02	1.487	1.035	1.451	<b>0.986</b>	1.036	1.040
WA	SMAPE	<b>11.671</b>	11.807	11.740	13.474	12.473	11.892	13.639	11.829	13.130	<b>11.698</b>	12.840	11.927
	MASE	<b>1.536</b>	1.590	1.575	1.866	1.677	1.608	2.095	1.585	1.896	<b>11.556</b>	1.701	1.613
	OWA	<b>0.832</b>	0.851	0.845	0.985	0.898	0.859	1.051	0.851	0.980	<b>0.838</b>	0.918	0.861

1748 **G.3 IMPUTATION**  
 1749

1750 Table 25: The complete results for the **imputation task** are as follows: To assess model performance  
 1751 under varying degrees of missing data, we randomly masked time points at rates of 12.5%, 25%,  
 1752 37.5%, and 50%.

	Models	TVNet (Ours)	PatchTST (2022)	SCINet (2022a)	Crossformer (2023)	RLinear (2023a)	MTS-Mixer (2023b)	DLinear (2023)	TimesNet (2022a)	MICN (2023)	ModernTCN (2024)	FEDformer (2022)	RMLP (2023a)		
Metrics	MSE	MAE	MSE	MAE	MSE	MAE	MSE	MAE	MSE	MAE	MSE	MAE	MSE	MAE	
ETTm1	12.5%	<b>0.014</b>	<b>0.078</b>	0.041	0.128	0.031	0.116	0.037	0.137	0.043	0.134	0.058	0.162	0.019	0.092
	25%	<b>0.016</b>	<b>0.083</b>	0.043	0.130	0.036	0.124	0.038	0.141	0.061	0.157	0.051	0.147	0.080	0.193
	37.5%	<b>0.019</b>	<b>0.090</b>	0.044	0.133	0.041	0.134	0.041	0.142	0.077	0.175	0.060	0.160	0.103	0.219
	50%	<b>0.023</b>	<b>0.101</b>	0.050	0.142	0.049	0.143	0.047	0.152	0.096	0.195	0.070	0.174	0.132	0.248
ETTm2	Avg	<b>0.018</b>	<b>0.088</b>	0.045	0.133	0.039	0.129	0.041	0.143	0.070	0.166	0.056	0.154	0.093	0.207
	12.5%	<b>0.018</b>	<b>0.081</b>	0.025	0.092	0.023	0.093	0.044	0.148	0.026	0.093	0.062	0.166	0.018	0.080
	25%	<b>0.021</b>	<b>0.081</b>	0.027	0.095	0.026	0.100	0.047	0.151	0.030	0.103	0.030	0.103	0.020	0.085
	37.5%	<b>0.025</b>	<b>0.089</b>	0.029	0.099	0.028	0.105	0.044	0.145	0.034	0.133	0.033	0.110	0.022	0.091
ETTh1	50%	<b>0.024</b>	<b>0.091</b>	0.032	0.106	0.031	0.111	0.047	0.150	0.039	0.123	0.037	0.118	0.131	0.247
	Avg	<b>0.022</b>	<b>0.086</b>	0.028	0.098	0.027	0.102	0.046	0.149	0.032	0.108	0.032	0.107	0.096	0.208
	12.5%	<b>0.032</b>	<b>0.119</b>	0.094	0.199	0.089	0.202	0.099	0.218	0.098	0.206	0.097	0.209	0.151	0.267
	25%	<b>0.039</b>	<b>0.137</b>	0.119	0.225	0.099	0.211	0.125	0.243	0.123	0.229	0.115	0.226	0.180	0.276
ETTh2	37.5%	<b>0.051</b>	<b>0.156</b>	0.145	0.248	0.107	0.218	0.148	0.263	0.153	0.253	0.135	0.244	0.215	0.318
	50%	<b>0.064</b>	<b>0.168</b>	0.173	0.271	0.120	0.231	0.158	0.281	0.188	0.278	0.160	0.263	0.257	0.347
	Avg	<b>0.046</b>	<b>0.145</b>	0.133	0.236	0.104	0.216	0.132	0.251	0.141	0.242	0.127	0.236	0.201	0.306
	12.5%	<b>0.036</b>	<b>0.119</b>	0.057	0.150	0.061	0.161	0.103	0.220	0.057	0.152	0.061	0.157	0.100	0.216
Electricity	25%	<b>0.038</b>	<b>0.123</b>	0.062	0.158	0.062	0.162	0.110	0.229	0.062	0.160	0.065	0.163	0.127	0.244
	37.5%	<b>0.040</b>	<b>0.126</b>	0.068	0.168	0.065	0.169	0.129	0.246	0.068	0.168	0.070	0.171	0.158	0.256
	50%	<b>0.044</b>	<b>0.143</b>	0.076	0.179	0.069	0.172	0.148	0.265	0.076	0.179	0.078	0.181	0.183	0.299
	Avg	<b>0.039</b>	<b>0.127</b>	0.066	0.164	0.064	0.165	0.122	0.240	0.066	0.165	0.069	0.168	0.142	0.259
Weather	12.5%	<b>0.065</b>	<b>0.180</b>	0.073	0.188	0.073	0.185	0.068	0.181	0.079	0.199	0.069	0.182	0.092	0.216
	25%	<b>0.075</b>	<b>0.192</b>	0.082	0.200	0.081	0.198	0.079	0.198	0.085	0.233	0.083	0.202	0.118	0.247
	37.5%	<b>0.085</b>	<b>0.196</b>	0.097	0.217	0.090	0.207	0.087	0.203	0.131	0.262	0.097	0.218	0.144	0.276
	50%	<b>0.091</b>	<b>0.210</b>	0.110	0.232	0.099	0.214	0.098	0.212	0.160	0.291	0.108	0.231	0.175	0.278
Weather	Avg	<b>0.079</b>	<b>0.194</b>	0.091	0.209	0.086	0.201	0.083	0.199	0.119	0.246	0.089	0.208	0.132	0.259
	12.5%	<b>0.021</b>	<b>0.037</b>	0.029	0.049	0.028	0.047	0.036	0.092	0.029	0.048	0.033	0.052	0.039	0.084
	25%	<b>0.024</b>	<b>0.037</b>	0.031	0.053	0.029	0.050	0.035	0.088	0.032	0.055	0.034	0.056	0.048	0.089
	37.5%	<b>0.024</b>	<b>0.040</b>	0.034	0.058	0.031	0.055	0.035	0.088	0.036	0.062	0.037	0.060	0.057	0.091
Weather	50%	<b>0.028</b>	<b>0.041</b>	0.039	0.066	0.034	0.059	0.038	0.092	0.040	0.067	0.041	0.066	0.034	0.092
	Avg	<b>0.024</b>	<b>0.039</b>	0.033	0.057	0.031	0.053	0.036	0.090	0.034	0.058	0.036	0.058	0.027	0.044

1782    **G.4 CLASSIFICATION**

1783

1784    **Table 26: Performance comparison of various models on different datasets with accuracy metrics**  
 1785    **for classification.**

1786

Datasets / Models	RNN-based			Convolution-based			MLP-based			Transformer-based			<b>TVNet</b> (Ours)		
	LSTNet (2018)	LSSL (2021)	Rocket (2020)	SCINet (2022a)	TimesNet (2022a)	MICN (2023)	ModernTCN (2024)	DLinear (2023)	LightTS (2022)	MTS-Mixer (2023b)	FED. (2022)	PatchTST (2022)	Cross. (2023)	Flow. (2022b)	
EthanolConcentration	39.9	31.1	45.2	34.4	35.3	35.7	36.3	36.2	29.7	33.8	31.2	32.8	38.0	33.8	35.6
FaceDetection	65.7	66.7	64.7	68.9	65.2	68.6	70.8	68.0	67.5	70.2	66.0	68.3	68.7	67.6	71.2
Handwriting	25.8	24.6	58.8	23.6	25.5	32.1	30.6	27.0	26.1	26.0	28.0	29.6	28.8	33.8	32.7
Heartbeat	77.1	72.7	75.6	77.5	74.7	78.0	77.2	75.1	75.1	77.1	73.7	74.9	77.6	77.6	78.1
JapaneseVowels	98.1	98.4	96.2	96.0	94.6	98.4	98.8	96.2	96.2	94.3	98.4	97.5	99.1	98.9	98.9
PEMS-SF	86.7	86.1	75.1	83.8	85.5	89.6	89.1	75.1	88.4	80.9	80.9	89.3	85.9	86.0	88.9
SelfRegulationSCP1	84.0	90.8	90.8	92.5	86.0	91.8	93.4	87.3	89.8	91.7	88.7	90.7	92.1	92.5	93.7
SelfRegulationSCP2	52.8	52.2	53.3	57.2	53.6	57.2	60.3	50.5	51.1	55.0	54.4	57.8	58.3	56.1	60.5
SpokenArabicDigits	100.0	100.0	71.2	98.1	97.1	99.0	98.7	81.4	100.0	97.4	100.0	98.3	97.9	98.8	99.4
UWaveGestureLibrary	87.8	85.9	94.4	85.1	82.8	85.3	86.7	82.1	80.3	82.3	85.3	85.8	85.3	86.6	86.6
Average Accuracy	71.8	70.9	72.5	71.7	70.0	73.6	<b>74.2</b>	67.5	70.4	70.9	70.7	72.5	73.2	73.0	<b>74.6</b>

1797    **G.5 ANOMALY DETECTION**

1798

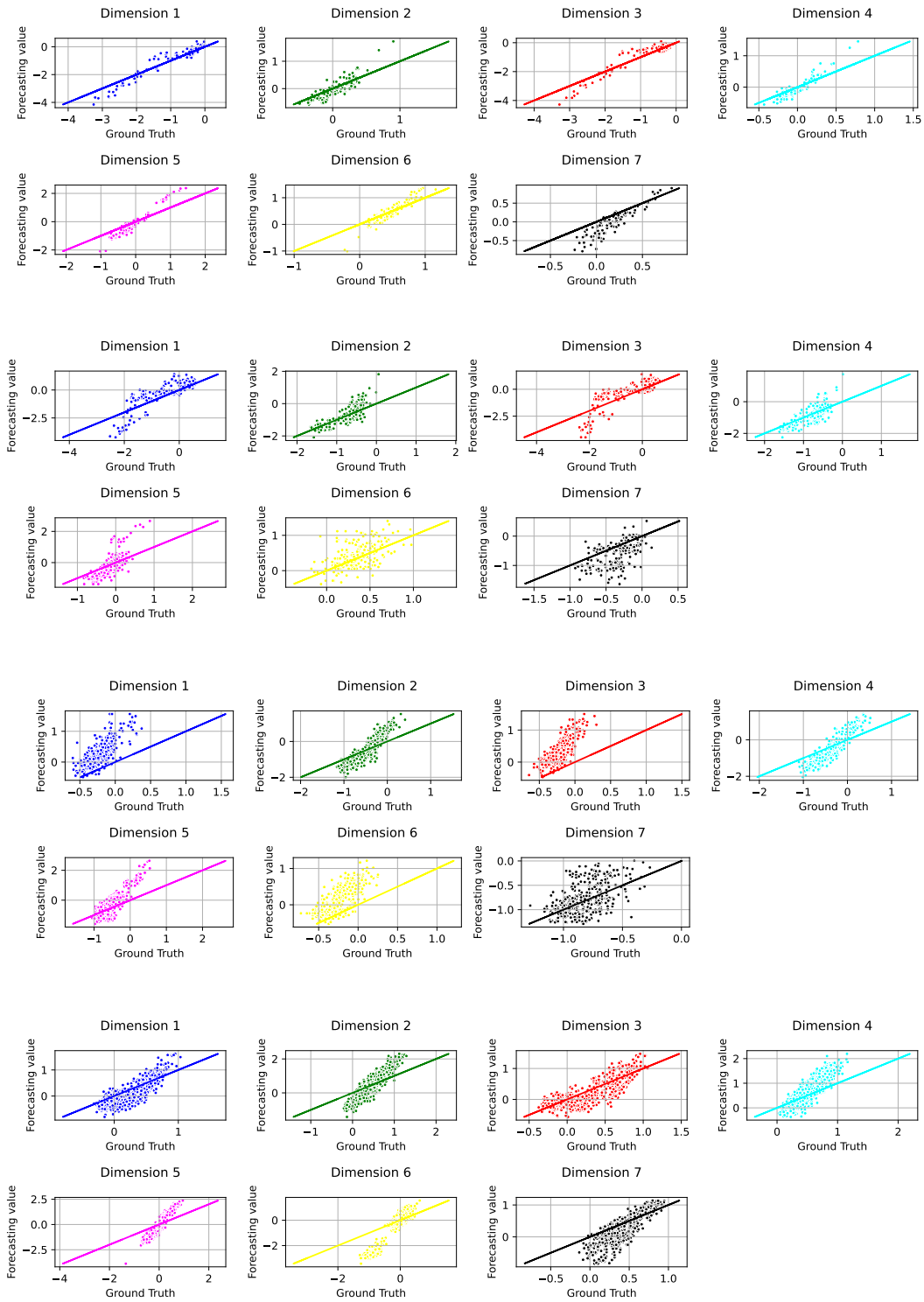
1800    **Table 27: Performance comparison of various models on different datasets with Precision (P), Recall**  
 1801    **(R), and F1-score (F1) metrics for anomaly detection.**

1802

Models	Datasets	SMD			MSL			SMAP			SWaT			PSM			Avg F1 (%)
		Metrics	P	R	F1												
SCINet	(2022a)	85.97	82.57	84.24	84.16	82.61	83.38	93.12	54.81	69.00	87.53	94.95	91.09	97.93	94.15	96.00	84.74
MICN	(2023)	88.45	83.47	85.89	83.02	83.67	83.34	90.65	61.42	73.23	91.87	95.08	93.45	98.40	88.69	93.29	85.84
TimesNet	(2022a)	88.66	83.14	85.81	83.92	86.32	85.15	92.52	58.29	71.52	86.76	97.32	91.74	98.19	96.76	97.47	86.34
DLinear	(2023)	83.62	71.52	77.10	84.34	84.52	84.88	92.32	55.41	69.26	80.91	95.30	87.52	98.28	89.26	93.55	82.46
LightsT	(2022)	87.10	78.42	82.53	82.40	75.78	78.95	92.58	55.27	69.21	91.98	94.72	93.33	98.37	95.97	97.15	84.23
MTS-Mixer	(2023b)	88.60	82.92	85.67	85.35	84.13	84.74	92.13	58.01	71.19	84.49	93.81	88.91	98.41	88.63	93.26	84.75
RLLinear	(2023a)	87.79	79.98	83.70	89.26	74.39	81.15	89.94	54.01	67.49	92.27	93.18	92.73	98.47	94.28	96.33	84.28
RMLP	(2023a)	87.35	78.10	82.46	86.67	65.30	74.48	90.62	52.22	66.26	92.32	93.20	92.76	98.01	93.25	95.57	82.31
Reformer	(2021)	82.58	69.24	75.32	85.51	83.31	84.40	90.91	57.44	70.40	72.50	96.53	82.80	59.93	95.38	73.61	77.31
Informer	(2021)	86.60	77.23	81.65	81.77	86.48	84.06	90.11	57.13	69.92	70.29	96.75	81.43	64.27	96.33	77.10	78.83
Anomaly*	(2021)	88.91	82.23	85.49	79.61	87.37	83.31	91.85	58.11	71.18	72.51	97.32	83.10	68.35	94.72	79.40	80.50
Pyraformer	(2021)	85.61	80.61	83.04	83.81	85.93	84.86	92.54	57.71	71.09	87.92	96.00	91.78	71/67	96.02	82.08	82.57
Autoformer	(2021)	88.06	82.35	85.11	77.27	80.92	79.05	90.40	58.62	71.12	89.85	95.81	92.74	99.08	88.15	93.29	84.26
Stationary	(2022b)	88.33	81.21	84.62	68.55	89.14	77.50	89.37	59.02	71.09	68.03	96.75	79.88	97.82	96.76	97.29	82.08
FEDformer	(2022)	87.95	82.39	85.08	77.14	80.07	78.57	90.47	58.10	70.76	90.17	96.42	93.17	97.31	97.16	97.23	84.97
Crossformer	(2023)	83.06	76.61	79.70	84.68	83.71	84.19	92.04	55.37	69.14	88.49	93.48	90.92	97.16	89.73	93.30	83.45
PatchTST	(2022)	87.42	81.65	84.44	84.07	86.23	85.14	92.43	57.51	70.91	80.70	94.43	87.24	98.87	93.99	96.37	84.82
ModernTCN	(2024)	87.86	83.85	85.81	83.94	85.93	84.92	95.17	57.69	71.26	91.83	95.98	93.86	98.09	96.38	97.23	<b>86.62</b>
TVNet	(Ours)	88.03	83.49	85.75	83.91	86.47	85.16	92.94	58.26	71.64	91.26	96.33	93.72	98.30	96.76	97.53	<b>86.76</b>

1821  
1822  
1823  
1824  
1825  
1826  
1827  
1828  
1829  
1830  
1831  
1832  
1833  
1834  
1835

1836 **H SHOWCASES**



1837  
1838  
1839  
1840  
1841  
1842  
1843  
1844  
1845  
1846  
1847  
1848  
1849  
1850  
1851  
1852  
1853  
1854  
1855  
1856  
1857  
1858  
1859  
1860  
1861  
1862  
1863  
1864  
1865  
1866  
1867  
1868  
1869  
1870  
1871  
1872  
1873  
1874  
1875  
1876  
1877  
1878  
1879  
1880  
1881  
1882  
1883  
1884  
1885  
1886  
1887  
1888  
1889

Figure 18: Visualization of ETTh1 Multivariate forecasting results

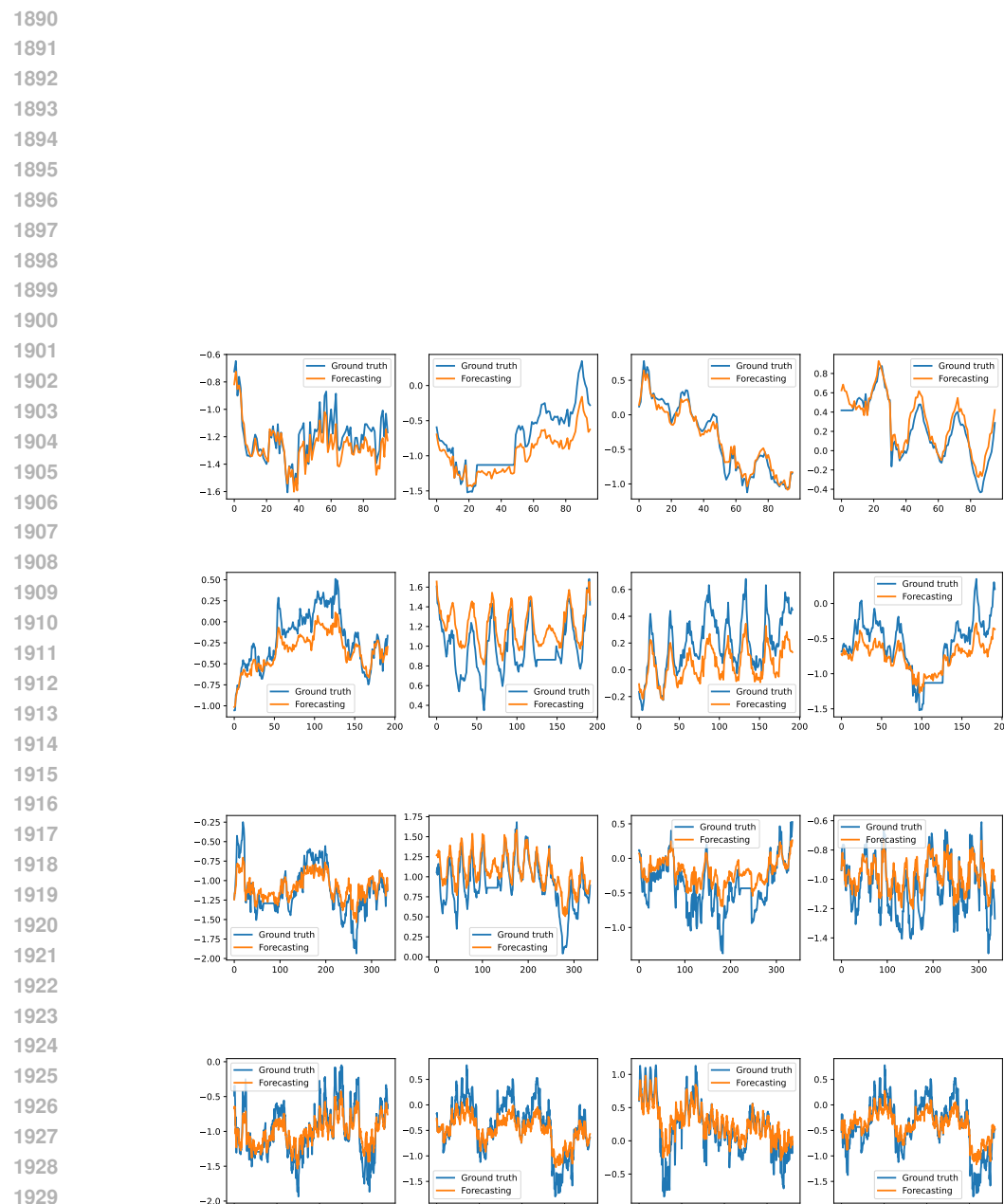


Figure 19: Visualization of ETTh1 Univariate forecasting results